Synthesis of $PtRe_2$ and Pt_2Re_2 Heterometallic Complexes from the Reaction of Dirhenium Carbonyl Compounds with Zerovalent Complexes of Platinum *

John Powell, John C. Brewer, Giulia Gulia and Jeffery F. Sawyer
Department of Chemistry, University of Toronto, Toronto, Ontario M5S 1A1, Canada

The monoacetonitrile complex $[Re_2(CO)_9(MeCN)]$, obtained from the reaction of $[Re_2(CO)_{10}]$ with freshly prepared iodosobenzene in acetonitrile solutions, reacts with the secondary phosphines PR_2H in refluxing hexane to give the complexes $[Re_2(CO)_9(PR_2H_2)]$ (**5a**, R = Ph; **5b**, R = Pr). Complexes **5**, when heated to >170 °C in decalin, lose CO and are converted cleanly to $[Re_2(\mu\text{-}PR_2)(\mu\text{-}H)(CO)_8]$ (**6a**, R = Ph; **6b**, R = Pr) while they react with $[Pt(C_2H_4)(PPh_3)_2]$ to give $[PtRe_2(\mu\text{-}PR_2)(\mu\text{-}H)(CO)_8(PPh_3)]$ (**7a**, R = Ph; **7b**, R = Pr), complexes containing a triangular $PtRe_2$ array with $Pt(\mu\text{-}PR_2)Re$, $Pt(\mu\text{-}H)Re$ and Re–Re edges. Similarly, reaction of complexes **5** with $[Pt(C_2H_4)_2\{P(C_6H_{11})_3\}]$ gives $[PtRe_2(\mu\text{-}PR_2)(\mu\text{-}H)(CO)_9\{P(C_6H_{11})_3\}]$ **8** containing $Pt(\mu\text{-}CO)Re$, $Pt(\mu\text{-}H)Re$ and $Re(\mu\text{-}PR_2)Re$ edges. The trimetallic complex **8** slowly disproportionates to give $[Re_2(\mu\text{-}PR_2)(\mu\text{-}H)(CO)_8]$ **6** and $\frac{1}{3}$ $[Pt_3(CO)_3\{P(C_6H_{11})_3\}_3]$. The reaction of **6a** ($\mu\text{-}PPh_2$) with $[Pt(C_2H_4)_2\{P(C_6H_{11})_3\}]$ gives the complex $[PtRe_2(\mu\text{-}PPh_2)(\mu\text{-}H)(CO)_8\{P(C_6H_{11})_3\}]$ **7c** in which the $\mu\text{-}PPh_2$ ligand has migrated from a ReRe edge in **6a** to a PtRe edge in **7**. Further reaction of **7c** with a second equivalent of $[Pt(C_2H_4)_2\{P(C_6H_{11})_3\}]$ yields the tetrametallic complex $[Pt_2Re_2(\mu\text{-}PPh_2)(\mu\text{-}H)(CO)_8\{P(C_6H_{11})_3\}_2]$ **10** ($\mu\text{-}PPh_2$, μ-H and 2μ-CO on PtRe edges). Reaction of $[Re_2(CO)_{10}]$ with $[Pt(C_2H_4)_2\{P(C_6H_{11})_3\}]$ gives $[PtRe_2(CO)_{10}\{P(C_6H_{11})_3\}]$ and $[Pt_2Re_2(CO)_{10}\{P(C_6H_{11})_3\}_2]$ **12** (4μ-CO on PtRe edges). The molecular structures of **7b**, **10** and **12** have been determined by single-crystal X-ray diffraction studies. Crystal data as follows: **7b**, orthorhombic, space group, *Pbca*, a = 14.951(2), b = 18.330(2), c = 25.715(2) Å, Z = 8, R = 0.0521 (R' = 0.0597) for 3700 data with $I \geqslant 3\sigma(I)$; **10**, monoclinic space group, $P2_1/n$, a = 15.215(9), b = 19.633(9), c = 19.446(8) Å, β = 92.90(4)°, Z = 4, R = 0.0950 (R' = 0.1006) for 6068 data with $I \geqslant {}^3\sigma(I)$; and **12**, triclinic (paramonoclinic) space group, $P\bar{1}$, a = 11.567(4), b = 15.308(6), c = 16.178(6) Å, α = 89.87(3), β = 108.13(3), γ = 90.28(3)°, Z = 2, R = 0.0659 (R' = 0.0716) for 7166 data with $I \geqslant 3\sigma(I)$.

Interest in metal–metal bonded compounds of the transition metals has focused in recent years on the elucidation of their structure, bonding, spectroscopic and catalytic properties.[1–7] Whilst the isolobal analogy[8] has provided considerable structural rationalization and resulted in the development of synthetic strategies that have led to a large increase in the quantity of data appertaining to heterometallic compounds, there have been relatively small gains in the understanding of reactivity patterns associated with these compounds. As a consequence, reactions of trimetallic compounds and compounds of higher metallic nuclearity are often unpredictable and rational synthetic design is rather restricted. With respect to elucidating reaction mechanisms in cluster systems mixed-metal clusters are particularly well suited to provide information with regard to (*i*) the effect of one metal centre on the reactivity of adjacent metal centres; (*ii*) details concerning the site(s) of chemical reaction; and (*iii*) the mechanism(s) of the cluster-assembly process. Considerable information relevant to these goals has been obtained from the utilization of phosphido bridge ligands in the development and study of new and chemically interesting heterometallic systems.[9–31]

A simple and effective (high yield) means of incorporating a *single* bridging phosphido group into a heterobimetallic dinuclear complex involves the reaction of a secondary phosphine-substituted metal carbonyl such as $[M(CO)_5(PR_2H)]$ (M = Cr, Mo or W), with a zerovalent platinum compound to

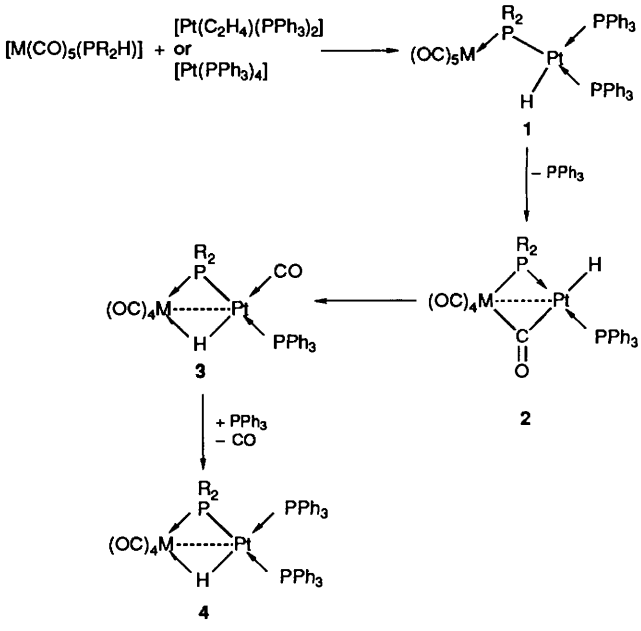

Scheme 1 Mechanism of platinum-assisted CO loss in the formation of $[(OC)_4M(\mu\text{-}PR_2)(\mu\text{-}H)Pt(PPh_3)_2]$. Whether or not there is a *direct* M–Pt bond in this compound is an open question with several studies concluding that metal-metal bonding in some doubly bridged binuclear systems is better discussed in terms of multicentred linkages between the metals and the bridging groups[32]

* *Supplementary data available:* see Instructions for Authors, *J. Chem. Soc., Dalton Trans.*, 1992, Issue 1, pp. xx–xxv.

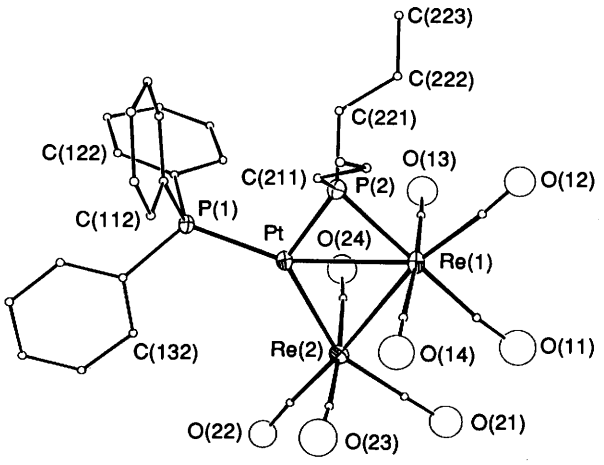

Fig. 1 The molecular structure of $[PtRe_2(\mu\text{-}PPr_2)(\mu\text{-}H)(CO)_8(PPh_3)]$ **7b**, the major product from the reaction of $[Re_2(CO)_9(PPr_2H)]$ with $[Pt(C_2H_4)(PPh_3)_2]$ [equation (5)]. The hydride ligand is presumed to bridge PtRe(2) – see text. Thermal ellipsoids are at the 25% probability level with the exception of C atom radii which are of arbitrary size

form phosphido-bridged bimetallic compounds containing a terminal platinum hydride, **1** (Scheme 1).[24,25] This species however, is very reactive and proceeds to decarbonylate readily in solution yielding the phosphido–hydrido bridged dinuclear compounds **4** as the final product. The mechanism for this reaction involves loss of PPh_3 from Pt of **1** and the formation of a bridging carbonyl intermediate **2**. Rearrangement of **2** to the μ-hydrido platinum carbonyl, **3**, is followed by facile substitution of the CO on Pt by PPh_3 to give the final μ-hydrido-μ-phosphido product **4**. The net effect is transfer of a carbonyl from an 18-electron metal centre (thermally substitutionally inert for monometallic systems) to a 16-electron square-planar Pt centre, which undergoes substitution with greater ease. Detailed spectroscopic studies of systems of the type shown in Scheme 1,[24,26] together with studies of the reactions of cationic secondary phosphine complexes such as $[W(cp)(CO)_3(PR_2H)]PF_6$[27] and $[Re(cp)(CO)(NO)(PR_2H)]BF_4$[28,29] (cp = η-$C_5H_5$) with $[Pt(C_2H_4)(PPh_3)_2]$ and $[Pt(C_2H_4)_2\{P(C_6H_{11})_3\}]$ have provided considerable insight into CO labilization and hydrogen-transfer reactions in phosphido-bridged heterobimetallic compounds.[30] Likewise spectroscopic studies of the reaction of $[Fe(CO)_4(PR_2H)]$ complexes with excess $[Pt(C_2H_4)_2\{P(C_6H_{11})_3\}]$ have provided useful information with regard to the reaction sequences and structural requirements for incorporation of $Pt\{P(C_6H_{11})_3\}$ in the synthesis of a range of $FePt$, $FePt_2$ and $FePt_3$ compounds.[31]

In view of the success of the approach to both the synthesis and detailed studies of phosphido-bridged MPt and MPt clusters we have attempted to extend the method to the synthesis of mixed-metal clusters of higher nuclearity containing M_2Pt_n and M_3Pt_n frameworks.[33] In its simplest form the approach requires the synthesis of monosubstituted secondary-phosphine complexes of di- and poly-nuclear metal carbonyls {*e.g.* $[M_2(CO)_9(PR_2H)]$ (M = Mn or Re); $[M_3(CO)_{11}(PR_2H)]$ (M = Ru or Os) *etc.*}. In this paper we report some initial studies in this area involving the synthesis of $[Re_2(CO)_9(PR_2H)]$ (R = Ph or Pr) and its reaction with $[Pt(C_2H_4)(PPh_3)_2]$ and $[Pt(C_2H_4)_2\{P(C_6H_{11})_3\}]$ to give $PtRe_2$ and Pt_2Re_2 products. The molecular structures of two of these derivatives have been determined by X-ray diffraction methods, along with the structure of a second Pt_2Re_2 cluster obtained from the reaction of $[Pt(C_2H_4)_2\{P(C_6H_{11})_3\}]$ with $[Re_2(CO)_{10}]$. Simplified *localized* bonding schemes are used to describe the $PtRe_2$ and Pt_2Re_2 products. Localized bonding models have proven particularly successful in *rationalizing* molecular geometries.[33–35]

Results

The acetonitrile complex eq-$[Re_2(CO)_9(MeCN)]$ is readily obtained in high yield (85–95%) from the reaction of $[Re_2(CO)_{10}]$ with freshly prepared iodosobenzene in acetonitrile solution [equation (1)]. The method can also be used to

$$[Re_2(CO)_{10}] + C_6H_5IO \xrightarrow[MeCN]{2\text{-}24h,\ 20\ ^\circ C} \text{eq-}[Re_2(CO)_9(MeCN)] \quad (1)$$

$$[Re_2(CO)_{10}] + \text{excess } C_6H_5IO \xrightarrow[MeCN]{2h,\ 20\ ^\circ C} [Re_2(CO)_8(MeCN)_2] \quad (2)$$

$$[Re_2(CO)_9(MeCN)] + PR_2H \xrightarrow[hexane]{reflux} \text{eq-}[Re_2(CO)_9(PR_2H)] \quad (3)$$

5a R = Ph
5b R = Pr

$$[Re_2(CO)_9(PR_2H)] \xrightarrow[decalin]{170\ ^\circ C} (OC)_4Re(\mu\text{-}PR_2)(\mu\text{-}H)Re(CO)_4 \quad (4)$$

5 → **6a** R = Ph; **6b** R = Pr

synthesise the disubstituted derivative $[Re_2(CO)_8(MeCN)_2]$ in 80% yield [equation (2)]. Treatment of eq-$[Re_2(CO)_9(MeCN)]$ with one equivalent of PR_2H (R = Ph or Pr) in refluxing hexane for 2–4 h gave the required complexes eq-$[Re_2(CO)_9(PR_2H)]$ (**5a**, R = Ph; **5b**, R = Pr) in 30–65% yield [equation (3)]. When $[Re_2(CO)_9(PR_2H)]$ **5** is heated in decalin (170 °C) for 30 min there is a clean conversion to the μ-phosphido-μ-hydrido complex $[Re_2(\mu\text{-}PR_2)(\mu\text{-}H)(CO)_8]$ (**6a**, R = Ph; **6b**, R = Pr) [equation (4)].[36] This reaction does *not* occur after 4 h of refluxing in toluene indicative of the relative inertness of $[Re_2(CO)_9(PR_2H)]$ **5** to thermal CO loss. Refluxing $[Re_2(CO)_8(MeCN)_2]$ with a molar equivalent of PPh_2H in hexane for 1 h gave **6a** as the major product together with several minor products, one of which is tentatively assigned to $[(OC)_4Re(\mu\text{-}PPh_2)(\mu\text{-}H)Re(PPh_2H)(CO)_3]$ (see Experimental section).

Reaction of $[Re_2(CO)_9(PR_2H)]$ *with* $[Pt(C_2H_4)(PPh_3)_2]$.—Addition of one equivalent of $[Pt(C_2H_4)(PPh_3)_2]$ to a CH_2Cl_2 solution of $[Re_2(CO)_9(PR_2H)]$ gives a deep orange solution from which orange crystals of a product with the stoichiometry $[PtRe_2(\mu\text{-}PR_2)(\mu\text{-}H)(CO)_8(PPh_3)]$ (**7a**, R = Ph; **7b**, R = Pr) may be isolated [equation (5)]. The structure of **7** is based on

$$[Re(CO)_9(PR_2H)] + [Pt(C_2H_4)(PPh_3)_2] \quad \mathbf{5}$$

$$\xrightarrow[-CO]{\sim 30min,\ 20\ ^\circ C,\ CD_2Cl_2} (OC)_4Re(\mu\text{-}H)(\mu\text{-}PR_2)Re(CO)_4Pt(PPh_3) + \mathbf{6}\ (minor) + [Pt(PPh_3)_3(CO)]\ (minor) \quad (5)$$

7a R = Ph
7b R = Pr

IR and ^1H and $^{31}P\text{-}\{^1H\}$ NMR data (Table 1) and a single-crystal X-ray diffraction study of **7b** (Fig. 1) (the utilization of a localized Re→Pt donor bond in the structural representation of **7** in Scheme 2 is discussed later, Fig. 7). When the reaction of $[Re_2(CO)_9(PR_2H)]$ **5** with $[Pt(C_2H_4)(PPh_3)_2]$ is monitored by ^1H NMR (hydrido region) and $^{31}P\text{-}\{^1H\}$ NMR spectroscopy it is found that the starting material is consumed in *ca.* 30 min (CD_2Cl_2, 20 °C) and that the reaction also results in the formation of $[Re_2(\mu\text{-}PR_2)(\mu\text{-}H)(CO)_8]$ **6** and possibly $[Pt(PPh_3)_3(CO)]$ [$^{31}P\text{-}\{^1H\}$ NMR: δ 9, $J(^{195}Pt^{31}P)$ 3720 Hz] as

Table 1 Proton and ^{31}P-{^1H} NMR data for the complexes $[PtRe_2(\mu\text{-}PR_2)(\mu\text{-}H)(CO)_8(PR_3)]$ **7**, $[PtRe_2(\mu\text{-}PR_2)(\mu\text{-}H)(\mu\text{-}CO)(CO)_8\{P(C_6H_{11})_3\}]$, **8** and $[Pt_2Re_2(\mu\text{-}PPh_2)(\mu\text{-}H)(\mu\text{-}CO)_2(CO)_6\{P(C_6H_{11})_3\}_2]$ **10** recorded in CD_2Cl_2 solution, J in Hz

Complex	**7a** (μ-PPh_2, PPh_3)	**7b** (μ-PPr_2, PPh_3)	**7c** [μ-PPh_2,$P(C_6H_{11})_3$]	**8a** (μ-PPh_2)	**8b** (μ-PPr_2)	**10**	
$\delta(\mu\text{-H})$	−5.75	−5.8	−6.8	−5.5	−5.5	−11.2	
$^1J(^{195}Pt^1H)$	800	813	796	525	528	762	
$^2J(^{31}P^1H)$	57,11	63,13	76,13	12,0	12,0	60,15	
$\delta(\mu\text{-P})$	235	227	223	130	103.4	248	
$^1J[^{195}Pt(\mu\text{-}^{31}P)]$	2106	2329	2437	52	60	2389	
$\delta(PR_3)$	49.6	51.0	72	76.0	76.8	71.0	70.6
$^1J(^{195}Pt^{31}P)$	3810	3738	3537	3070	3045	4574	3714
$^2J(^{195}Pt^{31}P)$	—	—	—	—	—	168	342
$^2J[^{31}P(\mu\text{-}^{31}P)]$	0	0	9	10	6	6	0
$^1J(^{31}P^{31}P)$	—	—	—	—	—	17	17

minor products. No intermediate species are observed. For $[Re_2(CO)_9(PPh_2H)]$ **5a** the reaction gives **7a** and **6a** in a *ca.* 9:1 ratio whilst reaction of $[Re_2(CO)_9(PPr_2H)]$ **5b** gives **7b** and **6b** in a *ca.* 7:3 ratio. The compound $[Re_2(\mu\text{-}PR_2)(\mu\text{-}H)(CO)_8]$ **6** can be crystallized from solution and identified by comparison of its spectroscopic properties with those of a known sample. This reaction [equation (5)] is another example of a facile platinum assisted CO labilization (loss) from an 18-electron metal centre from which thermal loss (substitution) is usually very slow. Since the $PtRe_2$ compound $[PtRe_2(\mu\text{-}PR_2)(\mu\text{-}H)(CO)_8(PPh_3)]$ **7** does not decompose in solution to give $[Re_2(\mu\text{-}PR_2)(\mu\text{-}H)(CO)_8]$ **6** and **6** does not react with $[Pt(C_2H_4)(PPh_3)_2]$ to give **7** (see below), it follows that **6** and **7** must be formed *via* different reaction pathways.

Reaction of $[Re_2(CO)_9(PR_2H)]$ *with* $[Pt(C_2H_4)_2\{P(C_6H_{11})_3\}]$.—In previous studies when the complexes $[M(CO)_5(PR_2H)]$ (M = Cr, Mo or W) were treated with $[Pt(C_2H_4)_2\{P(C_6H_{11})_3\}]$ the complexes $[(OC)_3M(\mu\text{-}PR_2)(\mu\text{-}H)Pt(CO)\{P(C_6H_{11})_3\}]$ {which are structural analogues of the proposed intermediate, **3**, in the formation of $[(OC)_4M(\mu\text{-}PR_2)(\mu\text{-}H)Pt(PPh_3)_2]$, Scheme 1} were obtained.[24,25] With the hope of identifying possible intermediates in the formation of $[PtRe_2(\mu\text{-}PR_2)(\mu\text{-}H)(CO)_8(PR_3)]$ [equation (5)] the reaction of $[Re_2(CO)_9(PR_2H)]$ **5** with a molar equivalent of $[Pt(C_2H_4)_2\{P(C_6H_{11})_3\}]$ was investigated. When $[Pt(C_2H_4)_2\{P(C_6H_{11})_3\}]$ was added to a solution of $[Re_2(CO)_9(PPh_2H)]$ **5a** in CH_2Cl_2 the solution immediately turned yellow-orange. Monitoring by ^1H NMR and IR spectroscopy showed that the reaction [equation (6)] was relatively slow, starting materials being fully consumed

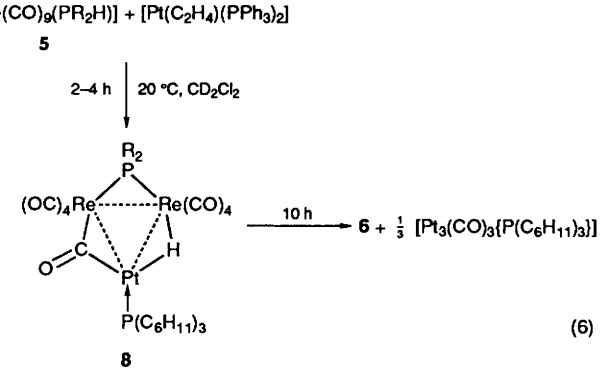

(6)

in 2–4 h. The ^1H NMR spectrum, within minutes of mixing, contained two hydridic species. One at δ −15.0 [$J(^{31}P^1H)$ 4.5 Hz] is readily assignable to $[Re_2(\mu\text{-}PPh_2)(\mu\text{-}H)(CO)_8]$ **6a**. The other signal consists of a 1:4:1 triplet of doublets at δ −5.5 [$J(^{31}P^1H)$ 12 and 0, $J(^{195}Pt^1H)$ 525 Hz] indicative of a Re-(μ-H)Pt moiety, which we assign to the trimetallic complex $[PtRe_2(\mu\text{-}PPh_2)(\mu\text{-}H)(\mu\text{-}CO)(CO)_8\{P(C_6H_{11})_3\}]$ **8a** [equation (6)]. The ^{31}P-{^1H} NMR spectrum within minutes of mixing exhibits resonances assignable to (*i*) complex **5a** and $[Pt(C_2H_4)_2\{P(C_6H_{11})_3\}]$ (as yet unreacted starting materials), (*ii*) to $[Re_2(\mu\text{-}PPh_2)(\mu\text{-}H)(CO)_8]$ **6a**, (*iii*) a complex pattern assignable to $[Pt_3(CO)_3\{P(C_6H_{11})_3\}]$, and (*iv*) two resonances at δ 130.0 [μ-PPh_2 ligand; $J(^{31}P^{31}P)$ 10, $J(^{195}Pt^{31}P)$ 52 Hz] and δ 76.0 [$P(C_6H_{11})_3$; $J(^{31}P^{31}P)$ 10, $J(^{195}Pt^{31}P)$ 3070 Hz] which are assignable to $[PtRe_2(\mu\text{-}PPh_2)(\mu\text{-}H)(\mu\text{-}CO)(CO)_8\{P(C_6H_{11})_3\}]$ **8a**. The small value of $J[^{195}Pt(\mu\text{-}^{31}P)]$ (52 Hz) is consistent with the phosphido group *bridging* the two Re atoms in the $PtRe_2$ complex **8a**. On standing, the signals assignable to $[Re_2(\mu\text{-}PPh_2)(\mu\text{-}H)(CO)_8]$ **6a** and $[Pt_3(CO)_3\{P(C_6H_{11})_3\}]$ grow in intensity, whilst the signals assignable to $[PtRe_2(\mu\text{-}PPh_2)(\mu\text{-}H)(\mu\text{-}CO)(CO)_8\{P(C_6H_{11})_3\}]$ **8a** eventually, after *ca.* 10 h, disappear. At the end of the reaction $[Re_2(\mu\text{-}PPh_2)(\mu\text{-}H)(CO)_8]$ **6a** and $[Pt_3(CO)_3\{P(C_6H_{11})_3\}]$ are readily isolated from the solution. {After 1 h of reaction several weak hydrido signals are observed which correspond to minor products from the reaction of **8a** with $[Pt(C_2H_4)\{P(C_6H_{11})_3\}]$ and of **6a** with $[Pt(C_2H_4)_2\{P(C_6H_{11})_3\}]$—see below.} The reaction of $[Re_2(CO)_9(PPr_2H)]$ **5b** with a molar equivalent of $[Pt(C_2H_4)_2\{P(C_6H_{11})_3\}]$ gives similar results (see Table 1 for spectroscopic data for **8b**). IR monitoring of the reaction (bridging carbonyl region) exhibits absorptions at 1764 cm^{-1} $\{[Pt_3(CO)_3\{P(C_6H_{11})_3\}]$ and weak bands at 1802 cm^{-1} (μ-PPr_2) and 1795 cm^{-1} (μ-PPh_2), which coincides with the lifetime of **8** in the reaction. An unusual feature of the formation of $[PtRe_2(\mu\text{-}PR_2)(\mu\text{-}H)(\mu\text{-}CO)(CO)_8\{P(C_6H_{11})_3\}]$ **8** [equation (6)] is the mechanism of insertion of μ-PR_2 across the two Re atoms. This is not observed in the reaction of $[Re_2(CO)_9(PR_2H)]$ with $[Pt(C_2H_4)(PPh_3)_2]$ to give **7**. However the formation of $[Re_2(\mu\text{-}PR_2)(\mu\text{-}H)(CO)_8]$ **6** in the reaction of $[Re_2(CO)_9(PR_2H)]$ with $[Pt(C_2H_4)(PPh_3)_2]$ [see equation (5)] *may* involve an intermediate structurally similar to **8**.

When $[Re_2(CO)_9(PPr_2H)]$ is treated with an *excess* of $[Pt(C_2H_4)_2\{P(C_6H_{11})_3\}]$ the reaction proceeds with initial formation of $[PtRe_2(\mu\text{-}PPr_2)(\mu\text{-}H)(\mu\text{-}CO)(CO)_8\{P(C_6H_{11})_3\}]$ **8b** [equation (6)] but now, over a period of hours, a new hydridic species corresponding to a Pt_2Re_2 cluster, **9**, is also observed. The ^1H NMR spectrum in the hydridic region exhibits a 1:1:1:1 quartet [δ_H −11.0, $J(^{31}P^1H)$ 44 and 15 Hz] with platinum satellites [$J(^{195}Pt^1H)$ 759 Hz (similar to **7**)]. The ^{31}P-{^1H} NMR spectrum contains a typical R_3PPt–$PtPR_3$ pattern [almost equivalent $P(C_6H_{11})_3$ ligands] together with a μ-PR_2 signal at δ 92.9 coupled to one $P(C_6H_{11})_3$ and one $Pt\{J(^{31}P^{31}P)$ 6, $J[^{195}Pt(\mu\text{-}^{31}P)]$ 52 Hz}. The chemical shift and $J(^{195}Pt^{31}P)$ values for the phosphido ligand are comparable to those of **8** and are consistent with it bridging the two Re atoms. A possible *tentative* structural assignment for this tetranuclear species is **9** which is almost an isomeric form of the cluster $[Pt_2Re_2(\mu\text{-}PPh_2)(\mu\text{-}H)(\mu\text{-}CO)_2(CO)_6(\{P(C_6H_{11})_3\}_2]$ **10**, isolated from the reaction of $[Re_2(\mu\text{-}PPh_2)(\mu\text{-}H)(CO)_8]$ **6a** with

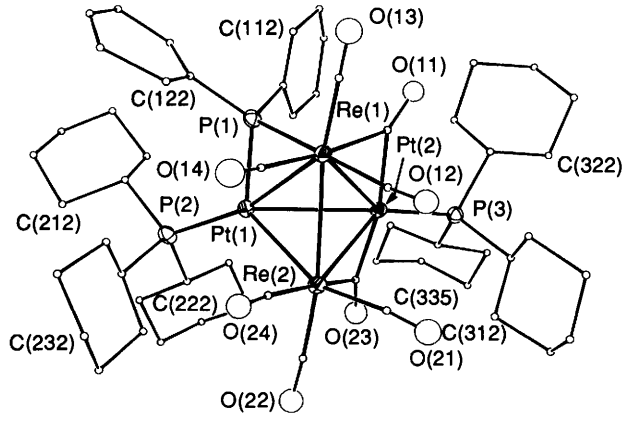

Fig. 2 The molecular structure of $[Pt_2Re_2(\mu\text{-}PPh_2)(\mu\text{-}H)(\mu\text{-}CO)_2(CO)_6\{P(C_6H_{11})_3\}_2]$ **10**, the major product of the reaction of $[Re_2(\mu\text{-}PPh_2)(\mu\text{-}H)(CO)_8]$ with an excess of $[Pt(C_2H_4)_2\{P(C_6H_{11})_3\}]$ [equations (7) and (8)]. The hydride ligand is presumed to bridge Pt(1)Re(2) – see text

excess $[Pt(C_2H_4)_2\{P(C_6H_{11})_3\}]$ [equation (8)]—see below and Fig. 2.

Reaction of $[Re_2(\mu\text{-}PR_2)(\mu\text{-}H)(CO)_8]$ *with* $[Pt(C_2H_4)_2\{P(C_6H_{11})_3\}]$.—It seemed possible that the $PtRe_2$ complex **8**, containing a $Re(\mu\text{-}PR_2)Re$ unit, could be the product of a reaction of $[Pt(C_2H_4)_2\{P(C_6H_{11})_3\}]$ with the $[Re_2(\mu\text{-}PR_2)(\mu\text{-}H)(CO)_8]$ **6** formed in reaction [equation (6)] as this would provide a possible explanation for the location of the phosphido bridge between the two rhenium atoms of **8**. Consequently we investigated the reaction of $[Re_2(\mu\text{-}PPh_2)(\mu\text{-}H)(CO)_8]$ **6a** with $[Pt(C_2H_4)_2\{P(C_6H_{11})_3\}]$ in CD_2Cl_2 at 20 °C [equation (7)]. The reaction proceeds *slowly* (*ca.* 80% of starting materials consumed in 24 h) to give initially the complex $[PtRe_2(\mu\text{-}PPh_2)(\mu\text{-}H)(CO)_8\{P(C_6H_{11})_3\}]$ **7c** containing a $Pt(\mu\text{-}PR_2)Re$ unit. The ^1H and $^{31}P\text{-}\{^1H\}$ NMR data are very similar to those of **7b** (see Table 1) the structure of which has been determined by X-ray diffraction (Fig. 1). This reaction *contrasts* with that of $[Pt(C_2H_4)_2\{P(C_6H_{11})_3\}]$ with $[Re_2(CO)_9(PR_2H)]$ **5** [equation (6)] in that the $\mu\text{-}PPh_2$ group that was initially bridging two Re atoms in $[Re_2(\mu\text{-}PR_2)(\mu\text{-}H)(CO)_8]$ now bridges Re–Pt in **7c**. When $[Re_2(\mu\text{-}PPh_2)(\mu\text{-}H)(CO)_8]$ **6a** and $[Pt(C_2H_4)_2\{P(C_6H_{11})_3\}]$ are allowed to react for 24 h, a second species assignable to the Re_2Pt_2 tetranuclear complex $[Pt_2Re_2(\mu\text{-}PPh_2)(\mu\text{-}H)(\mu\text{-}CO)_2(CO)_6\{P(C_6H_{11})_3\}_2]$ **10** [equation (8)] is evident in the spectroscopic data. The $^{31}P\text{-}\{^1H\}$ NMR signals corresponding to **10** contain a typical $(C_6H_{11})_3P\text{–}Pt\text{–}Pt\text{–}P(C_6H_{11})_3$ pattern, where the two phosphines are only slightly inequivalent, together with a phosphido signal at δ 248 [$J(^{195}Pt^{31}P)$ 2389] indicative of a $Pt(\mu\text{-}PPh_2)Re$ unit. Proton NMR spectroscopy indicates a $Pt(\mu\text{-}H)Re$ unit [δ_H −11.2; $J(^{195}Pt^1H)$ 762, $J(^{31}P^1H)$ 60 and 15 Hz]. The structural assignment of **10** [equation (8)] has been confirmed by a single-crystal X-ray diffraction study (see below and Fig. 2). It seems likely that $[Pt_2Re_2(\mu\text{-}PPh_2)(\mu\text{-}H)(\mu\text{-}CO)_2(CO)_6\{P(C_6H_{11})_3\}_2]$ **10** is formed from the reaction of $[PtRe_2(\mu\text{-}PPh_2)(\mu\text{-}H)(CO)_8\{P(C_6H_{11})_3\}]$ **7c** with $[Pt(C_2H_4)_2\{P(C_6H_{11})_3\}]$ [equation (8)].

The analogous reaction of $[Re_2(\mu\text{-}PPh_2)(\mu\text{-}H)(CO)_8]$ **6a** with $[Pt(C_2H_4)(PPh_3)_2]$ was investigated in order to ensure that **7a** is not formed from **5a** and $[Pt(C_2H_4)(PPh_3)_2]$ *via* the intermediacy of **6a**. After 24 h at room temperature, no *significant* reaction of **6a** with $[Pt(C_2H_4)(PPh_3)_2]$ was observed (IR, ^1H and $^{31}P\text{-}\{^1H\}$ NMR spectroscopy).

Reaction of $[Pt(C_2H_4)_2\{P(C_6H_{11})_3\}]$ *with* $[Re_2(CO)_{10}]$.—The possibility that the formation of the two $PtRe_2$ trinuclear complexes **7** [equation (5)] and **8** [equation (6)] involve two very different reaction pathways—namely initial oxidative

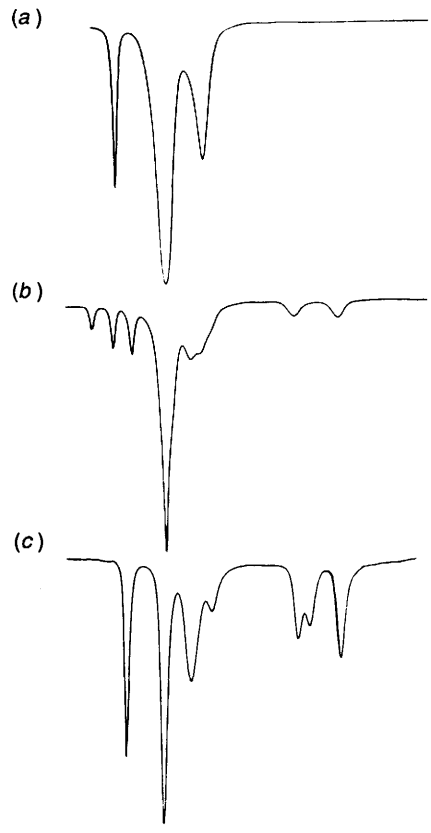

Fig. 3 IR[ν(CO) region] of CH_2Cl_2 solutions of (*a*) $[Re_2(CO)_{10}]$; (*b*) $[Re_2(CO)_{10}]$ + 1 equivalent of $[Pt(C_2H_4)_2\{P(C_6H_{11})_3\}]$ [*i.e.* complex **11**, equation (9)]; (*c*) $[Re_2(CO)_{10}]$ + 2 equivalents of $[Pt(C_2H_4)_2\{P(C_6H_{11})_3\}]$ [*i.e.* complex **12**, equation (10)]

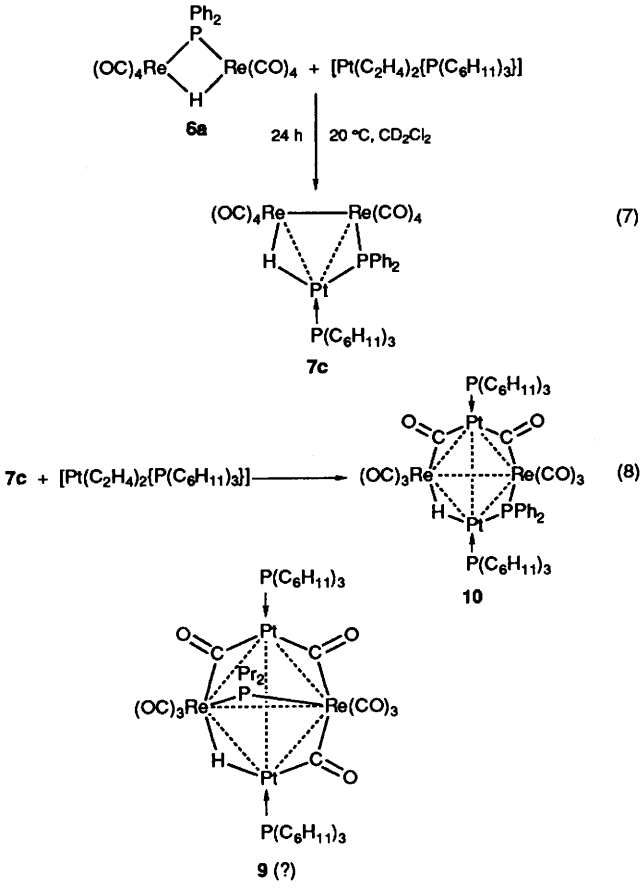

$[Re_2(CO)_{10}] + [Pt(C_2H_4)_2\{P(C_6H_{11})_3\}]$

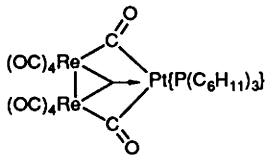

(9)

11

11 + $[Pt(C_2H_4)_2\{P(C_6H_{11})_3\}]$

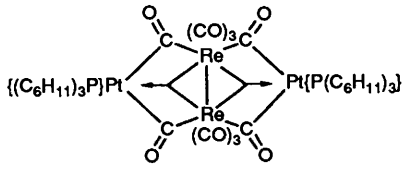

(10)

12

addition of P–H across Pt (formation of **7**) and initial addition of a $Pt(PR_3)$ fragment across an $Re_2(CO)_2$ moiety (formation of **8**)—was assessed further by an investigation of the reaction of $[Pt(C_2H_4)_2\{P(C_6H_{11})_3\}]$ with $[Re_2(CO)_{10}]$ in CH_2Cl_2 at 20 °C. IR monitoring [ν(CO) region—Fig. 3] indicates a rapid and quantitative reaction to form $[PtRe_2(CO)_{10}\{P(C_6H_{11})_3\}]$ **11** [equation (9)]. Addition of a further molar equivalent of $[Pt(C_2H_4)_2\{P(C_6H_{11})_3\}]$ to **11** results in the rapid formation of the complex $[Pt_2Re_2(CO)_{10}\{P(C_6H_{11})_3\}]$ **12** [equation (10)]. The presence of bridging carbonyl ligands is readily established by IR spectroscopy [Fig. 3: ν(μ-CO) (CH_2Cl_2 solution) 1856 and 1804 cm^{-1}, complex **11**; 1853, 1840 and 1802 cm^{-1}, complex **12**]. The $^{31}P-\{^1H\}$ NMR spectrum of **12** contains a typical $R_3PPtPtPR_3$ pattern [equivalent $P(C_6H_{11})_3$ ligands] and the molecular structure of **12** has been determined by single-crystal X-ray diffraction (see Fig. 4). The structure and formation of the triphenylphosphine analogue of **12** from the reaction of $[Re_2(CO)_{10}]$ with $[Pt(C_2H_4)(PPh_3)_2]$ in a stream of nitrogen has been recently reported.[37]

Discussion

The bimetallic carbonyl system required for this investigation was $[Re_2(CO)_9(PR_2H)]$. To overcome the problem of multiple substitution of CO by PR_2H and also avoid possible internal oxidative addition of the P–H bond of the PR_2H ligand across M–M bonds as an undesirable side reaction, a thermally mild synthetic route is required. Koelle[38] has previously synthesised the complexes $[Re_2(CO)_9L]$ (L = pyridine, acetonitrile, 2-methylpyridine or PPh_3) in good yield using the mild decarbonylating agent trimethylamine oxide[39] [equation (1)]. We have found freshly prepared iodosobenzene[40] to be particularly effective for both the mono- and di-substitution of $[Re_2(CO)_{10}]$ [equations (1) and (2)] giving isolated yields of eq-$[Re_2(CO)_9(MeCN)]$ (MeCN *trans* to CO) and $[Re_2(CO)_8(MeCN)_2]$ in the 80–90% range. The method is superior to that of Gard and Brown[41] who obtained the disubstituted product in 32% yield using trimethylamine oxide.

The reaction of PR_2H with $[Re_2(CO)_9(MeCN)]$ in refluxing hexane provided a mild route to the required precursor complexes eq-$[Re_2(CO)_9(PR_2H)]$ **5**. Assignments of configuration (equatorial or axial) based upon IR spectra are not particularly reliable for systems containing a large number of

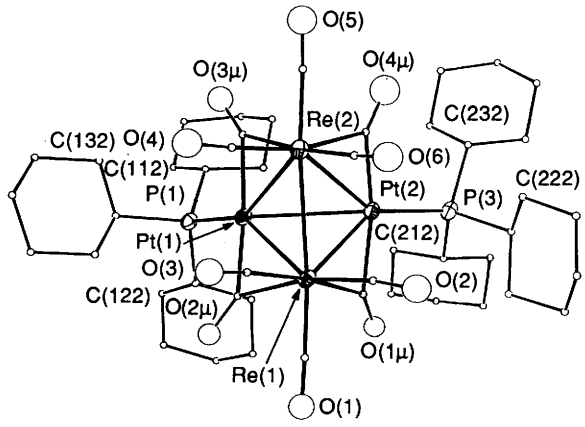

Fig. 4 The molecular structure of $[Pt_2Re_2(\mu\text{-}CO)_4(CO)_6\{P(C_6H_{11})_3\}_2]$ **12**

Table 2 Comparison of IR data [ν(CO) region, cm^{-1}] in hexane

$[Re_2(CO)_9(MeCN)]$	$[Re_2(CO)_9(PPh_2H)]$
2103w	2103w
2047m	2043m
2013m	2016m
1990vs	1995vs
1965m	1970m
1942m	1937m

carbonyl ligands. Examination of the IR data published for both isomers of $[Re_2(CO)_9(PPh_3)]$[42] does not resolve the problem as neither spectrum correlates well with that of $[Re_2(CO)_9(PPh_2H)]$. However based on the similarities of the IR data for eq-$[Re_2(CO)_9(MeCN)]$ and $[Re_2(CO)_9(PPh_2H)]$ (Table 2), the observed chemical reactions (see later) and a recent X-ray structural study of $[Mn_2(CO)_9(PPh_2H)]$,[43] we assign **5** to be the *equatorial* isomer. The presence of a co-ordinated PR_2H ligand is confirmed by ^1H and $^{31}P-\{^1H\}$ NMR spectroscopies [*e.g.* for **5a** $\delta_H(PH)$ 6.9, $J(^{31}P^1H)$ 362 Hz; $\delta_P = -12.6$ (upfield from 85% H_3PO_4)].

The ^1H NMR data (Table 1) for the $PtRe_2$ complexes **7** and **8** and the Pt_2Re_2 complex **10** support the location of the hydride as shown bridging Pt and Re. Whilst the $^1J(^{195}Pt^1H)$ values of *ca.* 750–800 Hz observed for **7** and **10** are at the high end of the range expected for bridging hydrides, the *trans* $^2J(^{31}P^1H)$ values of *ca.* 60–80 Hz are typical for bridging hydrides.[29,31,44] The large downfield ^{31}P chemical shift of the μ-PR_2 ligand (*ca.* 230 ppm) and large $J[^{195}Pt(\mu\text{-}^{31}P)]$ values (*ca.* 2200 Hz) imply an acute Re–P–Pt angle and a relatively short Re–Pt separation.[45] The Pt–μ-P distances in **7b** and **10** (2.236 and 2.211 Å) are slightly *shorter* than the Pt–PR_3 distances (2.243 and 2.273 Å respectively). However the $^1J(^{195}Pt^{31}P)$ couplings to the bridging μ-P are 35–45% smaller than those to the PR_3 ligands. A similar situation occurs in the cationic RePt dimers $[(cp)(ON)ReH(\mu\text{-}PR_2)Pt(PPh_3)_2]^+$ (R = C_6H_{11} or Ph) and has been ascribed to *decreased* s-orbital overlap and *bent* Pt–μ-P bonding in systems with acute M–μ-P–Pt bond angles.[29,30]

The reaction of $[Re_2(CO)_9(PR_2H)]$ with $[Pt(C_2H_4)(PPh_3)_2]$ to give $[PtRe_2(\mu\text{-}PR_2)(\mu\text{-}H)(CO)_8(PPh_3)]$ **7** is an example of a platinum-assisted CO labilization process. The mild conditions of CO loss in this reaction [equation (5)] contrast markedly with the very vigorous conditions required for thermal CO substitution [*e.g.* see equation (4)]. In view of previous studies of the mechanism of platinum-assisted CO labilization and loss from a thermally, substitutionally inert, 18-electron metal centre (Scheme 1)[24,25] a plausible mechanism for the formation of the $PtRe_2$ complex **7** from the reaction of $[Re_2(CO)_9(PR_2H)]$ **5** and $[Pt(C_2H_4)(PPh_3)_2]$ [equation (5)], is as shown in Scheme 2. A slow oxidative addition of the P–H bond of **5** to

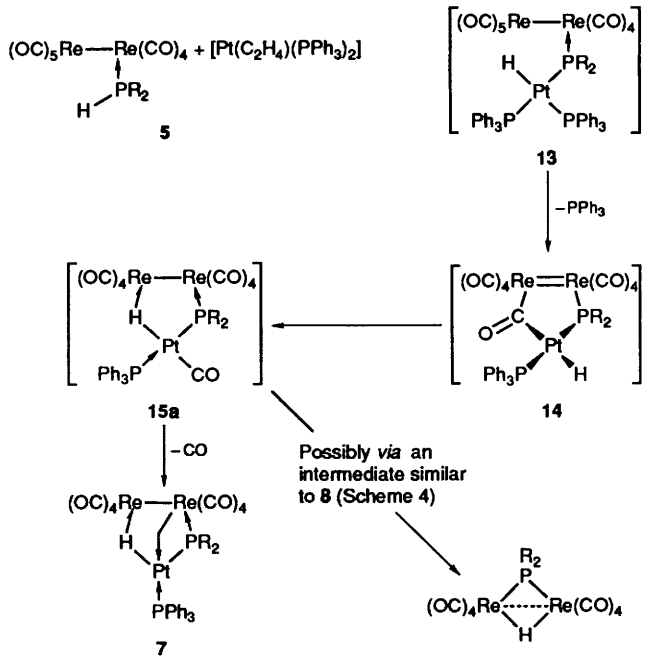

Scheme 2 A postulated reaction pathway for the formation of **7** and $[Re_2(\mu\text{-}PR_2)(\mu\text{-}H)(CO)_8]$ from the reaction of $[Re_2(CO)_9(PR_2H)]$ with $[Pt(C_2H_4)(PPh_3)_2]$

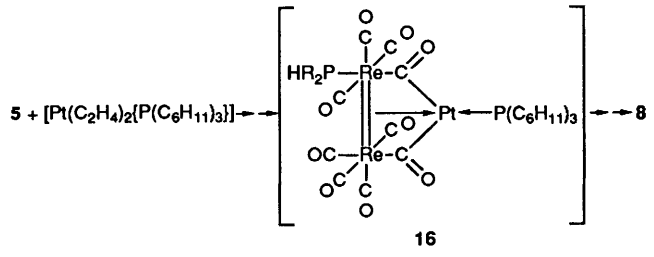

Scheme 3 A postulated intermediate species in the reaction of $[Pt(C_2H_4)_2\{P(C_6H_{11})_3\}]$ with $[Re_2(CO)_9(PR_2H)]$ **5**, if addition of $Pt\{P(C_6H_{11})_3\}$ to an $Re_2(CO)_2$ unit is the initial step. Contrast this to the reaction of **5** with $[Pt(C_2H_4)(PPh_3)_2]$ (Scheme 2) which is thought to involve an oxidative addition of the P–H bond as the initial step

$[Pt(C_2H_4)(PPh_3)_2]$ gives the terminal platinum hydride species **13** (not observed spectroscopically) which then labilizes a CO group from the $Re(CO)_5$ unit of **13** to give the μ-carbonyl species **14**. Interchange of the CO with the hydride ligand (as observed in the systems described in Scheme 1) converts **14** to **15** which, upon CO loss from Pt, gives the isolated $PtRe_2$ trimer **7**. Since **7** does not decompose to give $[Re_2(\mu\text{-}PR_2)(\mu\text{-}H)(CO)_8]$ **6**, the ready formation of **6** from **5** [equation (5)] must be platinum assisted and occur at a point prior to the formation of **7** *or by an entirely different mechanism.*

The reaction of $[Re_2(CO)_9(PR_2H)]$ **5** with $[Pt(C_2H_4)_2\{P(C_6H_{11})_3\}]$ is surprising in that it does *not* lead to the $PtRe_2$ trimer **7c**. Instead the only $PtRe_2$ species observed is the trimer **8** which requires the generation of a $Re(\mu\text{-}PPh_2)Re$ unit under very mild conditions [equation (6)]. Given that $[Pt(C_2H_4)_2\{P(C_6H_{11})_3\}]$ reacts rapidly with $[Re_2(CO)_{10}]$ to give the trimer **11** and the tetramer **12** [equations (9) and (10)] it is *probable* that the reaction of $[Re_2(CO)_9(PR_2H)]$ **5** with $[Pt(C_2H_4)_2\{P(C_6H_{11})_3\}]$ occurs *via* a similar pathway. Thus rapid addition of a $[Pt\{P(C_6H_{11})_3\}]$ unit across an $Re_2(CO)_2$ fragment of **5** would lead to the postulated intermediate **16** (Scheme 3) [structurally analogous to complex **11**, equation (9)] which subsequently rearranges to give **8** and then **6**. A similar reaction pathway may account for the formation of some **6** in equation (5).

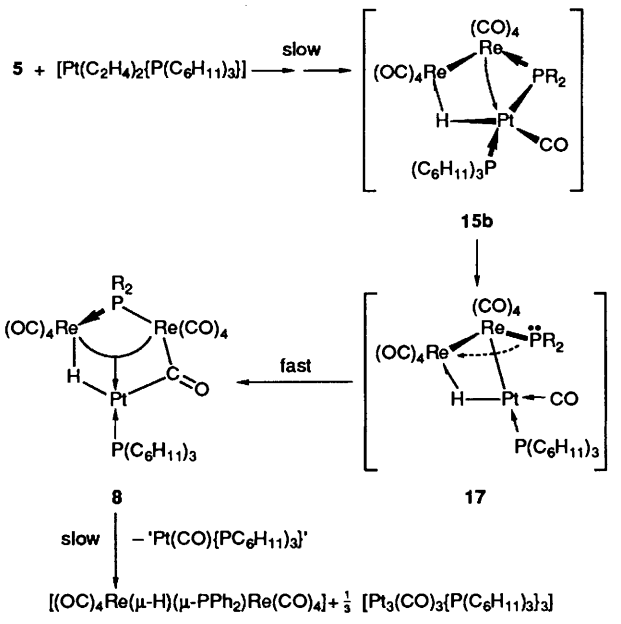

Scheme 4 An alternative mechanism to that in Scheme 3 in which the initial reaction of $[Re_2(CO)_9(PR_2H)]$ with $[Pt(C_2H_4)_2\{P(C_6H_{11})_3\}]$ is oxidative addition of P–H. The subsequent postulation of a bridge ⟶ terminal ⟶ bridge reorganization of the PR_2 ligand is analogous to experimentally observed bridge ⟷ terminal reorganization of a hydride ligand [Fig. 5(*c*)][26,29]

The addition of a $Pt\{P(C_6H_{11})_3\}$ unit across $Re_2(CO)_2$ fragments of $[Re_2(CO)_{10}]$ [equations (9) and (10)] provides credence to the postulated mechanism for the formation of **8** (Scheme 3). However the possibility that **8** is formed *via* initial oxidative addition of P–H across Pt followed by a subsequent rearrangement involving migration of a $\mu\text{-}PR_2$ from a PtRe to a ReRe site cannot be readily excluded. Indeed the lability of the $\mu\text{-}PR_2$ group in these systems is demonstrated by the fact that $[Re_2(\mu\text{-}PR_2)(\mu\text{-}H)(CO)_8]$ **6**, which is one of the end products of the reaction of $[Re_2(CO)_9(PR_2H)]$ **5** with $[Pt(C_2H_4)_2\{P(C_6H_{11})_3\}]$, *does* itself react with $[Pt(C_2H_4)_2\{P(C_6H_{11})_3\}]$ to give the $PtRe_2$ product **7c** in which the $\mu\text{-}PR_2$ ligand has *migrated* from an Re_2 bridge position in **6**, to an RePt bridge position in **7c**. These observations point to very stereospecific, kinetically controlled reaction pathways. {N.B. **7a** and **7b** *do not* form *via* initial formation of **6a** and **6b** on addition of $[Pt(C_2H_4)(PPh_3)_2]$ to **5** [equation (5)] since no reaction of **6** with $[Pt(C_2H_4)(PPh_3)_2]$ is observed even after 24 h}. Thus it may be that reaction of $[Re_2(CO)_9(PR_2H)]$ **5** with $[Pt(C_2H_4)_2\{P(C_6H_{11})_3\}]$ follows very closely the steps shown in Scheme 4 (similar to the formation of **15a** in Scheme 2) except that now the intermediate complex **15b** undergoes rearrangement *via* **17** to give **8** much faster than CO loss (which would give **7c**). It should be noted that the rearrangement **15b** ⟶ **17** (Scheme 4) involves a bridge-to-terminal rearrangement of the phosphido ligand which results in one of the Re atoms in **17** being in a formal valency state of III whilst the other is Re^{I} and the Pt atom exhibits a valency state of II. This *postulated* rearrangement of the phosphido ligand is analogous to the *observed* rearrangement of the hydrido ligand in the bridge-to-terminal hydride rearrangements reported for the isomeric pairs $[(OC)_3Fe(\mu\text{-}PR_2)(\mu\text{-}H)Pt(PPh_3)_2]$/$[(OC)_3HFe(\mu\text{-}PR_2)Pt(PPh_3)_2]$[26] and $[(cp)(ON)(OC)Re\{\mu\text{-}P(C_6H_{11})_2\}(\mu\text{-}H)Pt(PPh_3)_2^{+}]$/$[(cp)(ON)(OC)\text{-}HRe\{\mu\text{-}P(C_6H_{11})_2\}Pt(PPh_3)_2]^{+}$.[28,29] It should also be noted that the rate of the rearrangement of $[FePt_2(\mu\text{-}PR_2)(\mu\text{-}H)(\mu\text{-}CO)(CO)_3\{P(C_6H_{11})_3\}_2]$ **18** ($\mu\text{-}PR_2$ in an FePt site) to the isomeric form **19** ($\mu\text{-}PR_2$ in a PtPt site) [equation (11)] decreases in the order $\mu\text{-}P(C_6H_{11})_2 \gg \mu\text{-}PPh_2 > \mu\text{-}PPr_2$. This

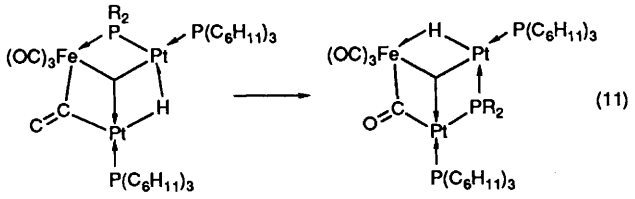

18 19

suggests a Fe–μ-P dissociative step in the reorganization of **18** to **19**[31] involving a bridge ⟶ terminal ⟶ bridge rearrangement of the PR_2 ligand similar to that postulated in Scheme 4.

Once CO loss *has* occurred, the preferred structure for a $PtRe_2$ system is probably that found in **7**. Consequently the reaction of $[Re_2(\mu\text{-}PR_2)(\mu\text{-}H)(CO)_8]$ **6** with $[Pt(C_2H_4)_2\{P(C_6H_{11})_3\}]$ leads to $[PtRe_2(\mu\text{-}PR_2)(\mu\text{-}H)(CO)_8\{P(C_6H_{11})_3\}]$ **7c**. This reaction [equation (7)] involves the migration of the PR_2 ligand from an Re_2 bridge position to a PtRe bridge position. The lability of the Re centres to μ-PR_2 and μ-CO reorganization in the $PtRe_2$ systems is quite remarkable in view of the usual inertness of $[Re_2(CO)_{10-x}L_x]$ systems to ligand substitution. Whilst the currently available data are insufficient fully to delineate the mechanism(s) of the rearrangements reported here, these results, and previous more definitive studies of the mechanism of formation and solution structures of $[(OC)_xM(\mu\text{-}PR_2)(\mu\text{-}H)Pt(PR_3)_2]$ ($x = 4$, M = Cr, Mo or W; $x = 3$, M = Fe or Ru)[25,26] and $[(cp)(ON)Re(\mu\text{-}PR_2)(\mu\text{-}H)Pt(PR_3)_2]^+$[29] point to kinetically accessible isomeric structures involving a formal two-electron change in total valency state of an M or M_2 unit as the likely cause of the increased ligand lability/reactivity in M_xPt_y clusters in comparison to monomeric ML_z systems. Fig. 5 presents localized bonding models of these arrangements in which the Pt centre can be regarded as an intramolecular two-electron oxidizing agent with oxidation being initiated/accompanied by loss of ligand from the Pt centre. Recent results have shown chemical or electrochemical two-electron oxidations to be a highly effective means of activating ligand substitution of carbonyl cluster anions.[46] Also, in line with the above suggestion, Bradford *et al.*[47] have recently shown the phosphido bridge in $[Co_2Mo(cp)(\mu\text{-}PPh_2)(\mu_3\text{-}CC_6H_4Me)(CO)_6]^n$ ($n = +1, 0, -1$) to undergo a reversible two-electron oxidatively induced migration of the μ-PPh_2 ligand from a CoCo site to a CoMo site.

The Molecular Structures of $[PtRe_2(\mu\text{-}PPr_2)(\mu\text{-}H)(CO)_8(PPh_3)]$ **7b**, $[Pt_2Re_2(\mu\text{-}PPh_2)(\mu\text{-}H)(\mu\text{-}CO)_2(CO)_6\{P(C_6H_{11})_3\}_2]$ **10** *and* $[Pt_2Re_2(\mu\text{-}CO)_4(CO)_6\{P(C_6H_{11})_3\}_2]$ **12**.—Molecular structures and labelling schemes are given in Figs. 1, 2 and 4. Details of the structure determinations, bond lengths and bond angles are given in Tables 3–6. Complex **7b**, a 46-electron PtM_2 cluster, consists of a $PtRe_2$ triangle of metal atoms with the Pt–Re edges bridged by μ-PPh_2 and μ-H ligands. Although the position of the hydride ligand was not located, it can be inferred from the geometry of the Pt atom (see below). The structure of **7b** is similar in many respects to that of the recently reported complex $[PtRe_2(\mu\text{-}H)_2(CO)_8(PPh_3)_2]$.[48] The 58-electron clusters **10** and **12** are best described as butterfly clusters with no Pt–Pt bond and with the four Pt–Re edges bridged by CO ligands in the case of **12** and by two CO, one H and one PPh_2 ligand in **10**. Again the position of the μ-H ligand was not located and its position can only be inferred from the geometry about Pt. The molecule of **12**, which has approximate mirror symmetry, is structurally analogous to the PPh_3 derivative $[Pt_2Re_2(\mu\text{-}CO)_4(CO)_6(PPh_3)_2]$ recently reported by Ciani *et al.*[37]

In **7b** the Pt–Re distances differ significantly with the shorter [2.774(1) Å] involving the hydride-bridged edge. This distance is slightly longer than the Pt(μ-H)Re edge [2.761(2) Å] in **10**.

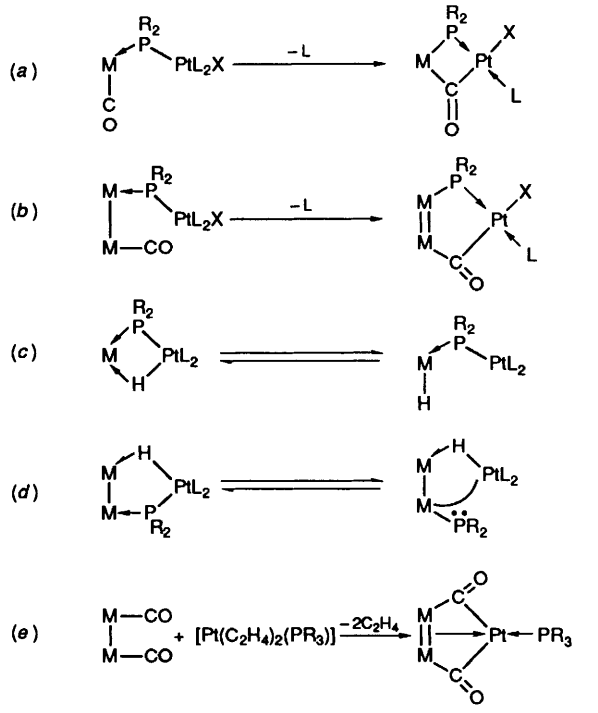

Fig. 5 Schematic representations (localized bonding models) of the two-electron change in total valency state of the M_xPt unit associated with CO labilization [(*a*) and (*b*)] and ligand-rearrangement processes [(*c*) and (*d*)]; (*e*) is an example of a four-electron change. Reactions (*a*) and (*c*) are well established.[26,29] Similar rearrangements have been postulated to occur in the μ-hydrido-μ-hydroxy species $[Re_2H(OH)(CO)_8]$, an intermediate in the photochemical reaction of $[Re_2(CO)_{10}]$ with H_2O[41]

Likewise, the Pt(μ-P)Re edge in **7b** [2.834(1) Å] is slightly longer than the corresponding edge in **10** [2.813(2) Å]. All of these distances are longer than the lengths of the remaining two Pt(μ-CO)Re edges in **10** and all four Pt(μ-CO)Re edges in **12** which average *ca.* 2.745 Å. Comparable Pt–Re distances in previously reported phosphido bridged structures are 2.8675(5) $\{[(cp)(ON)HRe\{\mu\text{-}P(C_6H_{11})_2\}Pt(PPh_3)_2]^+\}$, 2.8815(8) $\{[(cp)(ON)Re\{\mu\text{-}P(C_6H_{11})_3\}(\mu\text{-}H)Pt(PPh_3)_2]^+\}$ and 2.8673(4) Å $\{[(cp)(ON)Re(\mu\text{-}PPh_2)(\mu\text{-}H)Pt(PPh_3)_2]^+\}$.[29] The Pt–Re distance in $[(cp)(OC)_2HRe\text{–}PtH(PPh_3)_2]$ is 2.838(1) Å[49] whilst those in $[PtRe_2(\mu\text{-}H)_2(CO)_8(PPh_3)_2]$ are 2.906(1) (μ-H bridged) and 2.788(1) Å (no bridging ligand) respectively.[48]

The Re–Re distances in **7b**, **10** and **12** are 3.176(1), 3.149(2) and 3.0560(9) Å respectively, slightly longer than the nominal single-bond lengths of 3.041(1) Å in $[Re_2(CO)_{10}]$ (in which the equatorial CO ligands are staggered)[50] and distances of 2.956–3.024(7) Å in $[Re_4(CO)_{16}]^{2-}$.[51]

Typically Pt–Pt single bonds are 2.62–2.76 Å in length.[52,53] Both Pt–Pt distances in **10** [3.159(2) Å] and **12** [3.0417(8) Å] are therefore quite long but are similar to distances observed in the Pt_2M_2 butterfly clusters $[Pt_2Co_2(CO)_8(PPh_3)_2]$, $[Pt_2Fe_2(\mu\text{-}H)_2(CO)_8(PPh_3)_2]$, $[Pt_2Fe_2(\mu\text{-}H)(\mu\text{-}CO)_3(CO)_5(PPh_3)]^-$ and $[Pt_2Os_2(\mu\text{-}H)_2(CO)_8(PPh_3)_2]$ where the Pt–Pt distances are in the range 3.00–3.21 Å.[54,55] In **7** and **10** and the above Pt_2M_2 butterfly clusters the Pt · · · Pt distances represent only *weak* interactions which presumably arise from geometrical constraints imposed by other metal–ligand covalent bonding and the preponderance of square-planar arrangements of ligands about Pt. In all the compounds considered the fourth Pt orbital is either involved in a direct (unbridged) Pt–M metal–metal bond or else points towards the bond between the other heteroatoms in the cluster (*e.g.* Fig. 6). Whilst this interaction could be considered to be a three centre–two electron system, as has been commented upon for $[Cr(CO)_5\{Os(CO)_3(PMe_3)\}_2]$ and other systems[56] a slightly different analysis is given later in

Table 3 Crystal data,[a] details of intensity measurements and structure refinements

Compound	$C_{32}H_{30}O_8P_2PtRe_2$ **7b**	$C_{56}H_{77}O_8P_3Pt_2Re_2$ **10**	$C_{46}H_{66}O_{10}P_2Pt_2Re_2{\cdot}CH_2Cl_2$ **12**
M	1172.03	1733.73	1688.5
Crystal system	Orthorhombic	Monoclinic	Triclinic (paramonoclinic)
Space group	*Pbca*	$P2_1/n$	$P\bar{1}$
a/Å	14.951(2)	15.215(9)	11.567(4)
b/Å	18.330(2)	19.633(9)	15.308(6)
c/Å	25.715(2)	19.446(8)	16.178(6)
α/°	90	90	89.87(3)
β/°	90	92.90(4)	108.13(3)
γ/°	90	90	90.28(3)
U/Å^3	7047	5801	2722
$F(000)$	4352	3312	1600
$Z(D_c$/g cm$^{-3})$	8 (2.209)	4 (1.984)	2 (2.060)
μ(Mo-K$\bar{\alpha}$)/cm^{-1}	110.9	92.1	98.7
No. reflections for cell determination	25	24	24
θ range	9.6–16.7	10.6–16.6	9.3–14.6
Scan range/°	0.65 + 0.35 tanθ	0.80 + 0.35 tanθ	0.60 + 0.35 tanθ
Maximum scan time/s	70	60	55
No. standard reflections (interval/s)	3 (8500)	3 (7000)	2 (5500)
Decline in intensity standards (%)	0.9 (157.2 h)	11.2 (211.5 h)	14.0 (180.3 h)
Maximum linear decay correction	—	1.44	1.21
Quadrants (maximum 2θ/°)	h,k,l (52)	$h,k,\pm l$ (50)	$h,k,\pm l$ (55), $h,k,\pm l$ (50)
No. data collected (including standards)	8024[b]	11 990[c]	11 920
No. non-zero data	5975[d]	9125[e]	10 180[f]
Crystal colour and shape	Yellow fragment	Orange-red plate	Orange block
Crystal size (faces) d/cm	(010) 0.0050, (0$\bar{1}$0) 0.0150, (012) 0.0088, (0$\bar{1}$2) 0.0075, (0$\bar{1}\bar{2}$) 0.001 20, {100} 0.0050	(201) ($\bar{2}$0$\bar{1}$) 0.0021, (20$\bar{1}$) ($\bar{2}$01) 0.0081, (22$\bar{1}$) ($\bar{2}\bar{2}$1) 0.0088, (2$\bar{2}$1) ($\bar{2}$21) 0.0088	(011) (0$\bar{1}\bar{1}$) 0.0065, (01$\bar{1}$) (0$\bar{1}$1) 0.0072, (010) 0.0060, (0$\bar{1}$0) 0.0062, (10$\bar{1}$) ($\bar{1}$01) 0.0100
Absorption correction grid	6 × 10 × 12	6 × 10 × 10	12 × 6 × 8
Minimum, maximum transmission	0.170, 0.357	0.186, 0.587	0.128, 0.379
No. data $I > 3\sigma(I)$	3700	6068	7166
R (R')	0.0521 (0.0597)	0.0950 (0.1006)	0.0659 (0.0716)
Maximum Δ/σ in final cycle	0.232	0.051	
Value of p in weighting scheme[g]	0.007 08	0.006 58	0.005 47
Maximum peaks (e Å^{-3}) in final Fourier difference map	1.4 [near 0(23)], 1.3 [near 0(11)]	5.9 [near Pt(1)],[h] 4.7 [near Re(2)]	3.4–4.4 (near Pt and Re)

[a] Enraf-Nonius CAD4 diffractometer (graphite monochromator); Mo-K$\bar{\alpha}$ radiation (λ = 0.710 69 Å); T = 298 K; ω–2θ data collection mode. [b] Problems with the X-ray beam shutter resulted in some unsymmetrical backgrounds and incorrect scan speeds for some reflections. One particular block of data (121 reflections) was recollected at the end of the data collection and 6 reflections with bad $w\Delta F^2$ values were later rejected from the least-squares refinements. [c] Total includes 762 low angle data with 2$\theta \leqslant 35°$ and negative h and k indices. [d] 1653 Zero F_{obs} or systematically absent data rejected and 147 symmetry-equivalent data averaged (R merge = 0.042) to give indicated total. [e] 1509 Zero F_{obs} or systematically absent data rejected and 1011 symmetry-equivalent data averaged [R merge = 0.070 (0.107) for the absorption corrected (uncorrected) data] to give indicated total. [f] Total includes 252 standards. 966 Zero F_{obs} data rejected and 522 symmetry-equivalent data averaged [R merge = 0.020 (0.081) for the absorption corrected (uncorrected) data] to give the indicated total. [g] Weights given by $w = [\sigma^2(F) + pF^2]^{-1}$. [h] Somewhat high due to unfavourable shape of crystal and the resulting large absorption corrections.

Table 4 Selected bond lengths (Å) and bond angles (°) for $[PtRe_2(\mu\text{-}PPr_2)(\mu\text{-}H)(CO)_8(PPh_3)]$ **7b**

Pt–Re(1)	2.834(1)	Re(1)–Re(2)	3.176(1)	P(1)–C(111)	1.80(2)	Re(2)–C(23)	1.91(3)
Pt–Re(2)	2.774(1)	Re(1)–C(11)	1.87(3)	P(1)–C(121)	1.84(2)	Re(2)–C(24)	1.99(3)
Pt–P(1)	2.243(4)	Re(1)–C(12)	1.90(2)	P(1)–C(131)	1.81(2)	P(2)–C(211)	1.85(2)
Pt–P(2)	2.236(5)	Re(1)–C(12)	1.94(3)	Re(2)–C(21)	1.88(3)	P(2)–C(221)	1.84(2)
Re(1)–P(2)	2.417(5)	Re(1)–C(14)	1.97(3)	Re(2)–C(22)	1.90(2)		
Re(1)–Pt–Re(2)	68.98(3)	C(111)–P(1)–C(131)	102.1(7)	Re(2)–Re(1)–C(11)	76.7(10)	Re(1)–Re(2)–C(21)	97.4(8)
Re(1)–Pt–P(1)	157.0(1)	C(121)–P(1)–C(131)	102.8(7)	Re(2)–Re(1)–C(12)	166.8(7)	Re(1)–Re(2)–C(22)	174.9(6)
Re(1)–Pt–P(2)	55.4(1)	Pt–P(2)–Re(1)	74.9(2)	Re(2)–Re(1)–C(13)	87.6(6)	Re(1)–Re(2)–C(23)	88.6(7)
Re(2)–Pt–P(1)	133.8(1)	Pt–P(2)–C(211)	118.3(7)	Re(2)–Re(1)–C(14)	88.0(8)	Re(1)–Re(2)–C(24)	89.0(7)
Re(2)–Pt–P(2)	124.4(1)	Pt–P(2)–C(221)	118.5(7)	C(11)–Re(1)–C(12)	90.2(12)	C(21)–Re(2)–C(22)	87.6(10)
P(1)–Pt–P(2)	101.6(2)	Re(1)–P(2)–C(211)	120.5(7)	C(11)–Re(1)–C(13)	92.5(11)	C(21)–Re(2)–C(23)	92.3(11)
Pt–Re(1)–Re(2)	54.61(2)	Re(1)–P(2)–C(221)	118.5(8)	C(11)–Re(1)–C(14)	88.7(12)	C(21)–Re(2)–C(24)	93.5(11)
Pt–Re(1)–P(2)	49.6(1)	C(211)–P(2)–C(221)	104.8(10)	C(12)–Re(1)–C(13)	91.6(9)	C(22)–Re(2)–C(23)	90.1(10)
P(2)–Re(1)–Re(2)	104.2(1)	Pt–Re(1)–C(11)	131.2(10)	C(12)–Re(1)–C(14)	93.1(11)	C(22)–Re(2)–C(24)	91.9(10)
Pt–Re(2)–Re(1)	56.41(2)	Pt–Re(1)–C(12)	138.6(7)	C(13)–Re(1)–C(14)	175.1(10)	C(23)–Re(2)–C(24)	174.0(10)
Pt–P(1)–C(111)	113.4(5)	Pt–Re(1)–C(14)	87.7(8)	Pt–Re(2)–C(21)	153.7(8)	Pt–Re(1)–C(13)	87.9(6)
Pt–P(1)–C(121)	112.4(6)	P(2)–Re(1)–C(12)	88.9(7)	Pt–Re(2)–C(22)	118.6(6)	P(2)–Re(1)–C(11)	178.7(9)
Pt–P(1)–C(131)	118.4(5)	P(2)–Re(1)–C(14)	90.3(8)	Pt–Re(2)–C(23)	89.5(7)	P(2)–Re(1)–C(13)	88.5(6)
C(111)–P(1)–C(121)	106.3(8)			Pt–Re(2)–C(24)	84.5(7)		

Table 5 Selected bond lengths (Å) and bond angles (°) for $[Pt_2Re_2(\mu\text{-}PPh_2)(\mu\text{-}H)(\mu\text{-}CO)_2(CO)_6\{P(C_6H_{11})_3\}_2]$ **10**

Pt(1)–Pt(2)	3.159(2)	Pt(2)–Re(1)	2.748(2)	Re(1)–P(1)	2.471(9)	Re(2)–C(21)	1.90(3)
Pt(1)–Re(1)	2.813(2)	Pt(2)–Re(2)	2.750(2)	Re(1)–C(11)	2.13(2)	Re(2)–C(22)	1.86(3)
Pt(1)–Re(2)	2.761(2)	Pt(2)–P(3)	2.314(8)	Re(1)–C(12)	1.93(3)	Re(2)–C(23)	2.25(3)
Pt(1)–P(1)	2.211(7)	Pt(2)–C(11)	2.05(2)	Re(1)–C(13)	1.87(3)	Re(2)–C(24)	1.95(4)
Pt(1)–P(2)	2.273(8)	Re(1)–Re(2)	3.149(2)	Re(1)–C(14)	1.92(3)	Pt(2)–C(23)	1.90(3)
Pt(2)–Pt(1)–Re(1)	54.42(4)	Pt(2)–P(3)–C(311)	109.8(10)	Pt(1)–Re(1)–Pt(2)	69.23(4)	C(12)–Re(1)–C(14)	94.1(13)
Pt(2)–Pt(1)–Re(2)	54.87(4)	Pt(2)–P(3)–C(321)	114.7(10)	Pt(1)–Re(1)–Re(2)	54.83(4)	C(13)–Re(1)–C(14)	93.9(13)
Pt(2)–Pt(1)–P(1)	86.6(2)	Pt(2)–P(3)–C(331)	112.6(10)	Pt(1)–Re(1)–P(1)	48.9(2)	Pt(1)–Re(2)–Pt(2)	69.94(4)
Pt(2)–Pt(1)–P(2)	144.1(2)	Pt(1)–Pt(2)–Re(1)	56.35(4)	Pt(1)–Re(1)–C(11)	101.4(6)	Pt(1)–Re(2)–Re(1)	56.37(4)
Re(1)–Pt(1)–Re(2)	68.80(4)	Pt(1)–Pt(2)–Re(2)	55.19(4)	Pt(1)–Re(1)–C(12)	127.5(8)	Pt(1)–Re(2)–C(21)	155.4(8)
Re(1)–Pt(1)–P(1)	57.4(2)	Pt(1)–Pt(2)–P(3)	150.8(2)	Pt(1)–Re(1)–C(13)	139.4(9)	Pt(1)–Re(2)–C(22)	114.8(8)
Re(1)–Pt(1)–P(2)	161.2(2)	Re(1)–Pt(2)–Re(2)	69.89(4)	Pt(1)–Re(1)–C(14)	82.7(9)	Pt(1)–Re(2)–C(23)	80.7(8)
Re(2)–Pt(1)–P(1)	125.8(2)	Re(1)–Pt(2)–P(3)	146.8(2)	Pt(2)–Re(1)–Re(2)	55.09(4)	Pt(1)–Re(2)–C(24)	94.6(11)
Re(2)–Pt(1)–P(2)	121.4(2)	Re(2)–Pt(2)–P(3)	135.3(2)	Pt(2)–Re(1)–P(1)	91.6(2)	Pt(2)–Re(2)–Re(1)	55.02(4)
P(1)–Pt(1)–P(2)	112.1(3)	Pt(2)–Re(2)–C(21)	92.1(9)	Pt(2)–Re(1)–C(11)	47.6(6)	Pt(2)–Re(2)–C(22)	126.5(8)
Pt(1)–Pt(2)–C(11)	92.8(7)	Re(2)–Pt(2)–C(11)	119.4(7)	Pt(2)–Re(1)–C(12)	80.6(8)	Pt(2)–Re(2)–C(23)	43.2(7)
Pt(1)–Pt(2)–C(23)	75.9(9)	Re(2)–Pt(2)–C(23)	54.1(9)	Pt(2)–Re(1)–C(13)	127.3(9)	Re(1)–Re(2)–C(21)	99.8(8)
Re(1)–Pt(2)–C(11)	50.2(7)	Pt(2)–Re(2)–C(24)	143.3(10)	Pt(2)–Re(1)–C(14)	138.5(9)	Re(1)–Re(2)–C(23)	96.3(7)
Re(1)–Pt(2)–C(23)	120.9(9)	Re(1)–Re(2)–C(22)	170.9(8)	Re(2)–Re(1)–P(1)	103.5(2)	Re(1)–Re(2)–C(24)	88.6(10)
C(11)–Pt(2)–C(23)	168.7(12)	Pt(1)–P(2)–C(211)	115.4(11)	Re(2)–Re(1)–C(11)	102.2(6)	Pt(1)–P(2)–C(231)	110.5(13)
P(3)–Pt(2)–C(11)	98.8(7)	Pt(1)–P(2)–C(221)	109.4(12)	Re(2)–Re(1)–C(12)	72.7(8)	C(21)–Re(2)–C(22)	89.2(11)
P(3)–Pt(2)–C(23)	91.2(9)	C(211)–P(2)–C(221)	109.8(16)	Re(2)–Re(1)–C(14)	83.9(9)	C(21)–Re(2)–C(23)	97.8(12)
Re(2)–Re(1)–C(13)	165.3(9)	C(211)–P(2)–C(231)	106.6(17)	P(1)–Re(1)–C(11)	87.1(7)	C(21)–Re(2)–C(24)	90.3(14)
Pt(1)–P(1)–Re(1)	73.6(2)	C(221)–P(2)–C(231)	104.5(17)	P(1)–Re(1)–C(12)	172.2(9)	C(22)–Re(2)–C(23)	83.7(11)
Pt(1)–P(1)–C(111)	118.0(10)	C(311)–P(3)–C(321)	103.8(13)	P(1)–Re(1)–C(13)	91.0(9)	C(22)–Re(2)–C(24)	90.0(13)
Pt(1)–P(1)–C(121)	120.4(10)	C(311)–P(3)–C(331)	104.8(14)	P(1)–Re(1)–C(14)	92.2(10)	C(23)–Re(2)–C(24)	169.6(13)
Re(1)–P(1)–C(111)	116.0(10)	C(321)–P(3)–C(331)	110.3(14)	C(11)–Re(1)–C(12)	87.1(11)	Pt(2)–C(11)–O(11)	137.0(20)
Re(1)–P(1)–C(121)	126.5(11)	Pt(2)–C(11)–Re(1)	82.1(8)	C(11)–Re(1)–C(14)	173.8(10)	Pt(2)–C(23)–Re(2)	82.7(11)
C(111)–P(1)–C(121)	101.9(14)	Re(1)–C(11)–O(11)	140.9(19)	C(12)–Re(1)–C(13)	93.0(12)	Re(2)–C(23)–O(23)	129.6(22)
C(11)–Re(1)–C(13)	80.0(11)	Pt(2)–C(23)–O(23)	147.7(25)				

Table 6 Selected bond lengths (Å) and bond angles (°) for $[Pt_2Re_2(\mu\text{-}CO)_4(CO)_6\{P(C_6H_{11})_3\}_2]$ **12**

Re(1)–Re(2)	3.0560(9)	Pt(1)–C(3μ)	2.031(18)	Re(1)–C(2)	1.900(17)	Re(2)–C(5)	1.885(20)
Pt(1)–Pt(2)	3.0417(8)	Pt(2)–Re(1)	2.7416(10)	Re(1)–C(3)	1.919(21)	Re(2)–C(6)	1.906(21)
Pt(1)–Re(1)	2.7473(8)	Pt(2)–Re(2)	2.756(1)	Re(1)–C(1μ)	2.215(20)	Re(2)–C(3μ)	2.213(17)
Pt(1)–Re(2)	2.7343(9)	Pt(2)–P(2)	2.315(5)	Re(1)–C(2μ)	2.199(14)	Re(2)–C(4μ)	2.155(25)
Pt(1)–P(1)	2.317(4)	Pt(2)–C(1μ)	2.063(17)	Re(2)–C(4)	1.910(21)	Pt(2)–C(4μ)	1.945(22)
Pt(1)–C(2μ)	1.982(15)	Re(1)–C(1)	1.878(17)				
Pt(2)–Pt(1)–Re(1)	56.26(2)	Pt(1)–Re(1)–Re(2)	55.91(2)	Pt(1)–Pt(2)–Re(1)	56.44(2)	Pt(1)–Re(2)–Re(1)	56.32(2)
Pt(2)–Pt(1)–Re(2)	56.70(2)	Pt(1)–Re(1)–C(1)	125.3(5)	Pt(1)–Pt(2)–Re(2)	56.01(2)	Pt(1)–Re(2)–C(4)	91.5(5)
Pt(2)–Pt(1)–P(1)	130.6(1)	Pt(1)–Re(1)–C(2)	146.5(5)	Pt(1)–Pt(2)–P(2)	144.6(1)	Pt(1)–Re(2)–C(5)	130.0(6)
Pt(2)–Pt(1)–C(2μ)	95.7(4)	Pt(1)–Re(1)–C(3)	91.8(5)	Pt(1)–Pt(2)–C(1μ)	81.4(4)	Pt(1)–Re(2)–C(6)	138.5(6)
Pt(2)–Pt(1)–C(3μ)	87.7(5)	Pt(1)–Re(1)–C(1μ)	86.2(4)	Pt(1)–Pt(2)–C(4μ)	88.5(6)	Pt(1)–Re(2)–C(3μ)	47.0(5)
Re(1)–Pt(1)–Re(2)	67.77(2)	Pt(1)–Re(1)–C(2μ)	45.6(4)	Re(1)–Pt(2)–Re(2)	67.54(3)	Pt(1)–Re(2)–C(4μ)	92.9(6)
Re(1)–Pt(1)–P(1)	144.8(1)	Pt(2)–Re(1)–Re(2)	56.46(2)	Re(1)–Pt(2)–P(2)	142.2(1)	Pt(2)–Re(2)–Re(1)	56.00(2)
Re(1)–Pt(1)–C(2μ)	52.4(4)	Pt(2)–Re(1)–C(1)	130.6(6)	Re(1)–Pt(2)–C(1μ)	52.6(5)	Pt(2)–Re(2)–C(4)	148.1(5)
Re(1)–Pt(1)–C(3μ)	120.6(5)	Pt(2)–Re(1)–C(2)	87.5(6)	Re(1)–Pt(2)–C(4μ)	118.5(8)	Pt(2)–Re(2)–C(5)	122.9(7)
Re(2)–Pt(1)–P(1)	147.5(1)	Pt(2)–Re(1)–C(3)	138.2(5)	Re(2)–Pt(2)–P(2)	146.2(1)	Pt(2)–Re(2)–C(6)	90.7(7)
Re(2)–Pt(1)–C(2μ)	118.4(4)	Pt(2)–Re(1)–C(1μ)	47.7(4)	Re(2)–Pt(2)–C(1μ)	119.4(5)	Pt(2)–Re(2)–C(3μ)	91.8(5)
Re(2)–Pt(1)–C(3μ)	52.9(5)	Pt(2)–Re(1)–C(2μ)	99.7(4)	Re(2)–Pt(2)–C(4μ)	51.1(7)	Pt(2)–Re(2)–C(4μ)	44.6(6)
P(1)–Pt(1)–C(2μ)	93.5(4)	Re(2)–Re(1)–C(1)	172.9(6)	P(2)–Pt(2)–C(1μ)	93.6(5)	Re(1)–Re(2)–C(4)	92.6(5)
P(1)–Pt(1)–C(3μ)	94.6(5)	Re(2)–Re(1)–C(2)	92.1(5)	P(2)–Pt(2)–C(4μ)	96.6(7)	Re(1)–Re(2)–C(5)	173.5(6)
C(2μ)–Pt(1)–C(3μ)	166.0(8)	Re(2)–Re(1)–C(3)	81.8(5)	C(1μ)–Pt(2)–C(4μ)	169.4(8)	Re(1)–Re(2)–C(6)	82.1(6)
Pt(1)–P(1)–C(111)	111.8(5)	Re(2)–Re(1)–C(1μ)	103.6(4)	Pt(2)–P(2)–C(211)	112.6(6)	Re(1)–Re(2)–C(3μ)	103.4(5)
Pt(1)–P(1)–C(121)	111.7(5)	Re(2)–Re(1)–C(2μ)	100.3(4)	Pt(2)–P(2)–C(221)	108.9(7)	Re(1)–Re(2)–C(4μ)	100.5(6)
Pt(1)–P(1)–C(131)	112.5(6)	C(1)–Re(1)–C(2)	87.7(7)	Pt(2)–P(2)–C(231)	113.6(7)	C(4)–Re(2)–C(5)	89.0(9)
C(111)–P(1)–C(121)	110.8(9)	C(1)–Re(1)–C(3)	91.2(8)	C(211)–P(2)–C(221)	105.8(9)	C(4)–Re(2)–C(6)	90.4(9)
C(111)–P(1)–C(131)	105.8(8)	C(1)–Re(1)–C(1μ)	83.5(7)	C(211)–P(2)–C(231)	112.5(10)	C(4)–Re(2)–C(3μ)	90.0(8)
C(121)–P(1)–C(131)	103.8(8)	C(1)–Re(1)–C(2μ)	80.0(6)	C(221)–P(2)–C(231)	102.6(8)	C(4)–Re(2)–C(4μ)	166.4(8)
Pt(2)–C(1μ)–Re(1)	79.6(6)	C(2)–Re(1)–C(3)	93.2(8)	Pt(1)–C(3μ)–Re(2)	80.1(6)	C(5)–Re(2)–C(6)	91.5(9)
Pt(2)–C(1μ)–O(1μ)	138.7(16)	C(2)–Re(1)–C(1μ)	92.9(8)	Pt(1)–C(3μ)–O(3μ)	140.7(15)	C(5)–Re(2)–C(3μ)	83.0(8)
Re(1)–C(1μ)–O(1μ)	141.2(14)	C(2)–Re(1)–C(2μ)	167.6(7)	Re(1)–C(3μ)–O(3μ)	138.4(16)	C(5)–Re(2)–C(4μ)	78.3(9)
Pt(1)–C(2μ)–Re(1)	82.0(5)	C(3)–Re(1)–C(1μ)	171.7(6)	Pt(2)–C(4μ)–Re(2)	84.3(8)	C(6)–Re(2)–C(3μ)	174.5(8)
Pt(1)–C(2μ)–O(2μ)	143.4(12)	C(3)–Re(1)–C(2μ)	88.1(7)	Pt(2)–C(4μ)–O(4μ)	141.0(21)	C(6)–Re(2)–C(4μ)	94.8(9)
Re(1)–C(2μ)–O(2μ)	133.5(12)	C(1μ)–Re(1)–C(2μ)	84.6(6)	Re(2)–C(4μ)–O(4μ)	134.6(19)	C(3μ)–Re(2)–C(4μ)	83.6(8)
Pt(1)–Re(1)–Pt(2)	67.30(2)	av. Re–C–O	174.8(15)	Pt(1)–Re(2)–Pt(2)	67.28(2)		

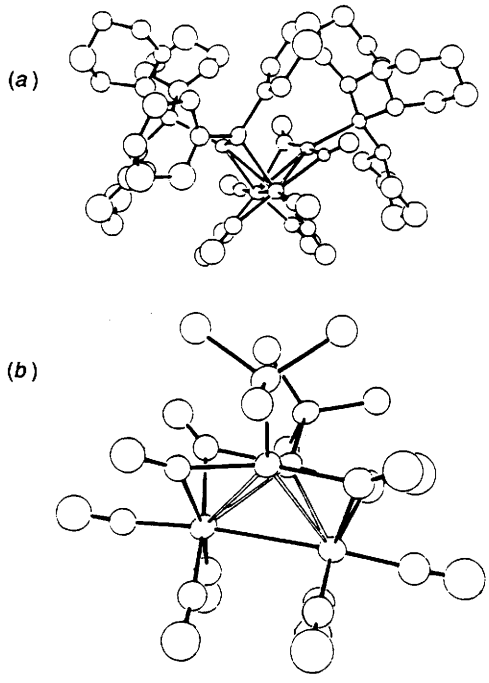

Fig. 6 Views of (*a*) molecule **10** virtually down the Re–Re axis, and (*b*) the core of molecule **12** with only the α-C atoms of the C_6H_{11} groups indicated for clarity, illustrating the molecular symmetry effectively imposed by the octahedral and square-planar fields at Re and Pt

this discussion. Fig. 6 is useful in that it readily indicates how the cluster **10** can be built-up from allowing the Pt(2)–$P(C_6H_{11})_3$ moiety to approach the $PtRe_2(\mu\text{-}P)(\mu\text{-}H)(CO)_8P$ fragment of **7b** across the Re–Re bond and between two of the out-of-plane carbonyls which become the bridging carbonyls C(11)–O and C(23)–O in the final product. Presumably the cluster **12** can be built up by a similar sequential addition of $PtP(C_6H_{11})_3$ moieties to $[Re_2(CO)_{10}]$. Fig. 6 also shows how the co-ordinative requirements of octahedral fields at Re and essentially four-co-ordinate planar fields at Pt *force* the eclipsed configuration of carbonyl ligands and the close proximity of the two Pt atoms in **10** and **12**. A similar analysis has been applied to the generation of a $PtRu_3$ cluster by the addition of a $Ru(CO)_2$ fragment across the Ru–Ru edge of a $[PtRu_2(\mu\text{-}PR_2)(\mu\text{-}H)(CO)_7]$ intermediate.[33]

Although not located in the X-ray structural studies the positions of the bridging hydrogen atoms in **7b** and **10** are inferred, from the geometrical parameters of the Pt and Re atoms involved, to be along the Pt–Re(2) edge in **7b** and along the Pt–Re(1) edge in **10** (consistent with solution ^1H NMR data). The Pt–Re distances are reasonably consistent with this in that the distances involved are somewhat longer than the distances for the Pt(μ-CO)Re edges but shorter than those for the Pt(μ-P)Re edges. It is commonly found in cluster structures that μ-CO bridged edges are usually shorter than unbridged edges and that hydride bridges generally tend to lengthen the M–M distance spanned although both of these observations have many exceptions.[57] If we assume (*i*) that the Pt–μ-H and Re–μ-H distances in **7** and **10** are close to the average value (1.75 and 1.85 Å) quoted by Teller and Bau[58] in their review of crystallographically determined transition-metal hydride structures and (*ii*) that the H atoms involved are in the planes of the bonds about Pt, then the resulting geometrical situation for **7b** is summarized in Fig. 7. Localized bonding models involving octahedral and square-planar fields at Re and Pt are particularly successful at rationalizing molecular geometries in the present structures. Using the P(1)–Pt vector as an estimate of the probable location of the fourth binding site in the planar ligand field at Pt suggests that, in **7b**, the Pt atom is more strongly bonded to Re(1) than Re(2) [see point B, Fig. 7(*a*)]. Also

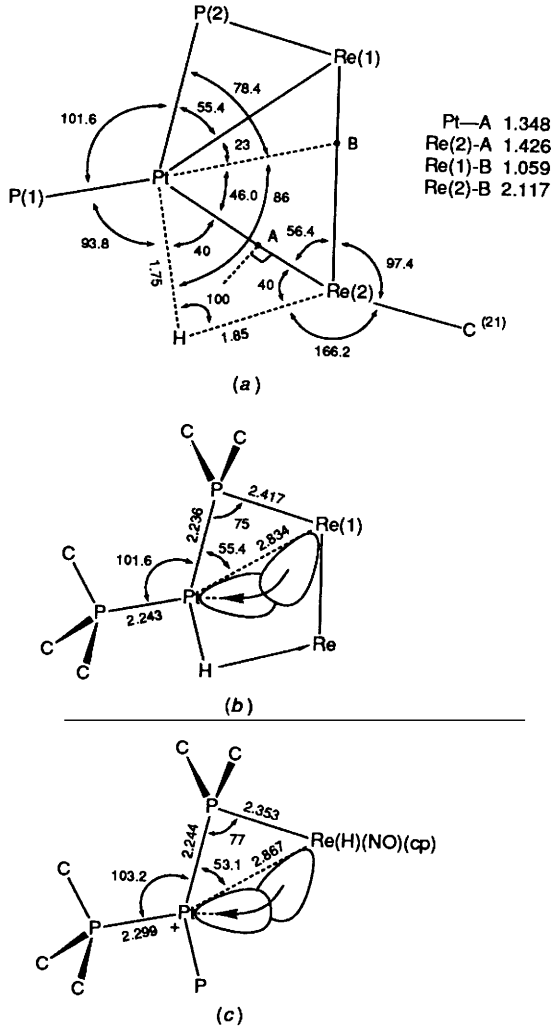

Fig. 7 (*a*) The geometrical situation for **7b** (bond lengths in Å, angles in °) assuming μ-H bridges PtRe(2) and is in the $PtRe_2$ plane with Pt–H 1.75 and Re–H 1.85 Å. (*b*) Also shown is a schematic with a Re(1)→Pt dative bond in the fourth Pt co-ordination site. (*c*) For a comparison with **7b** the structural features of the cation $[(cp)(ON)(OC)HRe\{\mu\text{-}P(C_6H_{11})_2\}Pt(PPh_3)_2]^+$[28,29] [analogous to those in (*b*)]. It is assumed that the Pt–μ-P interaction involves significant bending of the Pt–μ-P bond[29]

given in Fig. 7 is a simple representation of bent Re(1)→Pt donor bonding and an analogous description of the comparable features of the *directly bonded* PtRe bimetallic cation $[(Ph_3P)_2Pt\{\mu\text{-}P(C_6H_{11})_2\}ReH(NO)(cp)]^+$.[29] The similarity of the conformation, bond angles and bond lengths of the $(C_3P)Pt(\mu\text{-}PC_2)Re$ unit in both the bimetallic and trimetallic compounds supports the notion that in **7** the Pt is co-ordinated in the fourth site by an Re→Pt donor bond from the more basic Re(1) centre, presumably using a Re(1) filled t_{2g} type orbital. Similar dative metal–metal bonds have been postulated in $[(OC)_5W(\mu\text{-}PPh_2)Re(CO)_4]$,[17] $[(OC)_5W\{C(OMe)(C_6H_4OMe)\}Pt(PMe_3)_2]$,[59] and $[(Me_3P)(OC)_4Cr(\mu\text{-}PBu^t_2)NiCl(PMe_3)]$.[60]

Experimental

General.—All manipulations were carried out under an atmosphere of dry N_2 using dry degassed solvents. The $^{31}P\text{-}\{^1H\}$ and ^1H NMR spectra were recorded as CD_2Cl_2 solutions at room temperature on a Varian XL200 Fourier-transform NMR spectrometer operating at 80.9 and 200 MHz respectively. Proton shifts were measured relative to $SiMe_4$. Phosphorus-31 shifts were measured relative to external

$P(OMe)_3$ in C_6D_6 and corrected to 85% H_3PO_4, with downfield shifts reported as positive. Infrared data were obtained on a Nicolet 10DX Fourier-transform IR spectrometer. Samples were run as CH_2Cl_2 solutions in sodium chloride cells.

Starting Materials.—Dichlorodeuteriomethane was purchased from Aldrich and used as received. Metal carbonyl starting materials were purchased from Strem and Pressure Chemicals and used without further purification. Di-*n*-propylphosphine and diphenylphosphine were purchased from Strem and Pressure Chemicals, respectively. Trimethylamine oxide dihydrate and iodosobenzene diacetate were purchased from Aldrich. The platinum compounds $[Pt(C_2H_4)_2\{P(C_6H_{11})_3\}]$[61] and $[Pt(C_2H_4)(PPh_3)_2]$[62] were prepared according to published procedures. Iodosobenzene was prepared according to the method of Saltzman and Sharefkin.[63] The crude iodosobenzene was washed with acetonitrile, then diethyl ether and air dried. Yields were >90%. This material may be kept for short periods of time in a cool dark place. However, it is best prepared fresh when required.

Preparations.—*(Acetonitrile)nonacarbonyldirhenium*, eq-$[Re_2(CO)_9(MeCN)]$. In a typical preparation, $[Re_2(CO)_{10}]$ (3.16 g, 4.8 mmol) was dissolved in freshly distilled and degassed acetonitrile (225 cm^3). The flask was warmed slightly (≈40 °C) until the rhenium carbonyl was completely dissolved. Iodosobenzene, which was freshly prepared prior to use, was added (1.42 g, 6.4 mmol). The iodosobenzene was insoluble in acetonitrile. The suspension was left stirring for approximately 2 h at which point the IR spectrum of the cloudy yellow solution indicated the presence of some unreacted $[Re_2(CO)_{10}]$. An additional 0.24 g (1.09 mmol) iodosobenzene was added and the solution was left stirring overnight. The solvent was removed under reduced pressure, with the aid of a tepid water-bath, giving a beige-yellow solid. The product was recrystallized from methanol and water to give 2.5 g of $[Re_2(CO)_9(MeCN)]$. Yield 77%. IR (hexane): ν(CO) 2103w, 2047m, 2013m, 1990vs and 1965m cm^{-1}. (Isolated yields varied from 75 to 90%.)

Bis(acetonitrile)octacarbonyldirhenium, eq,eq-$[Re_2(CO)_8(MeCN)_2]$. Dirhenium decarbonyl (0.70 g, 1.07 mmol) was dissolved in freshly distilled, degassed MeCN (75 cm^3) and iodosobenzene [0.35 g plus, 0.39 g (after 1 h); 1.58 mmol, 1.76 mmol respectively] was added in portions. After stirring for 2 h the bright yellow solution was taken to dryness and washed with a minimum volume of hexane to yield the product as a yellow powder in 83% yield. This method is superior to that of Gard and Brown,[41] who obtained the product in 32% yield using trimethylamine oxide as the decarbonylating agent. IR (CH_2Cl_2): ν(CO) 2071w, 2016m, 1919s and 1905m cm^{-1}; impurities at 2054w and 2002m cm^{-1}. [Lit. (in MeCN):[41] 2070w, 2015m, 1962s and 1901m cm^{-1} with impurities at 2075 and 2001 cm^{-1} that could not be removed by chromatography or recrystallization of the material.]

Nonacarbonyl(diphenylphosphine)dirhenium, $[Re_2(CO)_9(PPh_2H)]$ **5a**. The complex $[Re_2(CO)_9(MeCN)]$ (0.65 g, 0.98 mmol) was placed in degassed hexane (*ca.* 150 cm^3) and diphenylphosphine (0.19 g, 1.03 mmol) was added. The mixture was refluxed in hexane for 2 h during which time the solution turned from yellow to colourless. The solvent was removed under pressure and washed with a minimum volume of methanol to give a chalk-white solid in 65% yield. The product may be recrystallized from a minimum volume of hot hexane as white microprisms. IR (benzene): ν(CO) 2103w, 2041m, 2016w, 1993vs, 1966m and 1931m. NMR (CD_2Cl_2): ^1H, δ 6.9 [$J(^{31}P^1H)$ 362 Hz, PH], 7.4 and 7.6 (complex, phenyl H); ^{31}P-$\{^1H\}$, δ −12.6 (Found: C, 31.3; H, 1.6. $C_{21}H_{11}O_9PRe_2$ requires C, 31.1; H, 1.4%).

*Nonacarbonyl(di-*n*-propylphosphine)dirhenium*, $[Re_2(CO)_9(PPr_2H)]$ **5b**. The complex $[Re_2(CO)_9(MeCN)]$ (0.91 g, 1.36 mmol) was dissolved in freshly distilled and degassed hexane (230 cm^3) and di-*n*-propylphosphine (0.18 cm^3, 1.38 mmol) was added by syringe. {The $[Re_2(CO)_9(MeCN)]$ was only slightly soluble in hexane.} The mixture was refluxed for 4 h after which the solvent was removed under reduced pressure to give a beige, sticky oil which recrystallized from hexane as off-white prisms (30% yield). IR (hexane): ν(CO) 2103w, 2039m, 1993vs, 1969m and 1938ms cm^{-1}. In addition there were weak unassigned bands at ν(CO) 2047, 2015, 1989 and 1978 cm^{-1}. NMR (CD_2Cl_2): ^1H, δ 4.9 [$J(^{31}P^1H)$ 344 Hz]; ^{31}P-$\{^1H\}$, δ −46.3 (s).

Octacarbonyl(μ-diphenylphosphido)(μ-hydrido)dirhenium, $[Re_2(\mu\text{-}PPh_2)(\mu\text{-}H)(CO)_8]$ **6a**. *Method A.* The complex $[Re_2(CO)_9(PPh_2H)]$ (0.086 g, 0.11 mmol) was placed in decalin (10 cm^3) and heated to 170 °C for 30 min, after which time the solution became a light orange colour. Solvent was removed under reduced pressure to give an off-white residue. IR (hexane): ν(CO) 2108w, 2085m, 2014vs, 2000m and 1965s cm^{-1}. NMR (CD_2Cl_2): ^1H, δ −14.9 [d, $J(^{31}P^1H)$ 4.5 Hz, ReH]; ^{31}P-$\{^1H\}$, 45.0 (s) (Found: C, 30.8; H, 1.7. $C_{20}H_{11}O_8PRe_2$ requires C, 30.7; H, 1.4%). Starting from $[Re_2(CO)_{10}]$ and carrying out the appropriate sequential reactions, but without isolation/purification of the intermediate products gave $[Re_2(\mu\text{-}PPh_2)(\mu\text{-}H)(CO)_8]$ in 45% overall yield.

Method B. The complex $[Re_2(CO)_8(MeCN)_2]$ (0.29 g, 0.43 mmol) was suspended in degassed hexane (75 cm^3) and diphenylphosphine (80 μl, 0.086 g, 0.46 mmol) was added. The mixture was refluxed for 1.25 h under nitrogen, filtered to remove insoluble material and the solvent removed under reduced pressure. An off-white material was obtained. The IR spectrum (hexanes) showed predominantly bands at 2108w, 2085m, 2015vs, 1999m and 1965s cm^{-1} corresponding to the desired product and minor bands attributed to impurities at 2099vw, 2043w, 1986m, 1915w and 1900w cm^{-1}. Proton and ^{31}P-$\{^1H\}$ NMR data for **6a** were as above. The major impurity tentatively assigned as $[(OC)_4Re(\mu\text{-}PPh_2)(\mu\text{-}H)Re(PPh_2H)(CO)_3]$ showed ^1H NMR signals at δ −13.4 [$J(^{31}P^1H)$ 7 and 13, ReH] and 7.7 [$J(^{31}P^1H)$ 481 Hz, PPh_2H]. The μ-PPr_2 analogue **6b** was prepared from **5b** *via* method A. NMR: ^1H, −15.14 [d, $J(^{31}P^1H)$ 7.0 Hz, ReH]; ^{31}P-$\{^1H\}$, δ 14.0.

$[PtRe_2(\mu\text{-}PPr_2)(\mu\text{-}H)(CO)_8(PPh_3)]$ **7b**. In the preparative reaction {from which product crystals of $[PtRe_2(\mu\text{-}PPr_2)(\mu\text{-}H)(CO)_8(PPh_3)]$ were isolated} $[Pt(C_2H_4)(PPh_3)_2]$ (0.24 g, 0.32 mmol) was added to a CH_2Cl_2 solution of $[Re_2(CO)_9(PPr_2H)]$ (0.23 g, 0.31 mmol). The solution immediately changed from colourless to pale orange. After stirring for 3 h at room temperature, the volume of solvent was reduced and methanol was added dropwise until the solution was just cloudy. On allowing the solution to stand undisturbed for several weeks at −20 °C, large orange crystals had formed which were suitable for an X-ray structure determination (Fig. 2). IR (CH_2Cl_2): ν(CO) 2081m, 2040m, 1988s, 1960m and 1919m cm^{-1}. The complex **7a** was similarly prepared. IR (hexane): ν(CO) 2084m, 2047m, 2015w, 1994vs, 1970m and 1933m cm^{-1} (Found: C, 36.70; H, 1.85. $C_{38}H_{26}O_8P_2PtRe_2$ requires C, 36.80; H, 2.10%).

Reaction of $[Re_2(CO)_9(PR_2H)]$ **5** *with* $[Pt(C_2H_4)_2\{P(C_6H_{11})_3\}]$. In a typical experiment $[Re_2(CO)_9(PPh_2H)]$ (0.077 g, 0.096 mmol) was dissolved in CD_2Cl_2 (0.5 cm^3) and $[Pt(C_2H_4)_2\{P(C_6H_{11})_3\}]$ (0.050 g, 0.095 mmol) was added (with stirring) as a solid. The solution is initially a pale yellow-orange colour but became deep red after 1–2 h with concurrent formation of crystalline $[Pt_3(CO)_3\{P(C_6H_{11})_3\}_3]$. The other major product, $[Re_2(\mu\text{-}PPh_2)(\mu\text{-}H)(CO)_8]$ **6a**, could be induced to crystallize from solution by addition of hexane. NMR (^1H and ^{31}P) spectra recorded in the first 2 h exhibited peaks attributable to the unstable trimeric species $[PtRe_2(\mu\text{-}PPh_2)(\mu\text{-}H)(\mu\text{-}CO)(CO)_8\{P(C_6H_{11})_3\}]$ **8a**, which diminished after a few hours and were totally absent after 24 h. Spectral data: (*i*) $[Pt_3(CO)_3\{P(C_6H_{11})_3\}_3]$, IR ($CH_2Cl_2$) 1763s cm^{-1}; ^{31}P-$\{^1H\}$ NMR δ 70.7 [$^1J(^{195}Pt^{31}P)$ 4382, $^2J(^{195}Pt^{31}P)$ 411, $^3J(^{31}P^{31}P)$ 56 Hz] [lit.,[64] ν(CO) 1770s cm^{-1}: δ_P 69.8 *J* 4412, 430 and 58 Hz]; (*ii*) $[PtRe_2(\mu\text{-}PPh_2)(\mu\text{-}CO)(CO)_8\{P(C_6H_{11})_3\}]$ **8a**, IR, ν(CO)

Table 7 Fractional atomic coordinates for complex **7b**

Atom	*X/a*	*Y/b*	*Z/c*	Atom	*X/a*	*Y/b*	*Z/c*
Pt	0.043 03(5)	0.237 76(4)	0.387 88(2)	C(114)	−0.222 1(14)	0.082 0(10)	0.509 5(7)
Re(1)	0.035 19(6)	0.202 97(4)	0.280 58(3)	C(115)	−0.133 9(14)	0.051 4(11)	0.512 0(7)
Re(2)	0.119 63(6)	0.347 24(4)	0.328 20(3)	C(116)	−0.059 9(12)	0.092 5(10)	0.505 5(7)
O(11)	0.096 5(18)	0.284 2(14)	0.182 2(10)	C(121)	0.126 3(13)	0.174 3(9)	0.502 2(6)
O(12)	−0.037 1(12)	0.076 8(10)	0.214 4(7)	C(122)	0.136 3(13)	0.164 2(10)	0.555 8(7)
O(13)	0.225 3(14)	0.134 7(11)	0.293 2(7)	C(123)	0.205 4(15)	0.129 3(12)	0.579 7(8)
O(14)	−0.147 7(15)	0.284 9(12)	0.275 9(8)	C(124)	0.276 3(16)	0.107 7(12)	0.543 3(9)
O(21)	0.188 9(15)	0.413 1(12)	0.225 2(9)	C(125)	0.270 2(15)	0.116 4(11)	0.494 0(8)
O(22)	0.189 3(12)	0.484 7(9)	0.380 8(7)	C(126)	0.197 4(13)	0.149 8(9)	0.469 7(7)
O(23)	−0.066 2(20)	0.418 9(15)	0.322 4(10)	C(131)	0.013 6(10)	0.298 2(8)	0.515 3(6)
O(24)	0.302 1(14)	0.265 7(11)	0.349 8(8)	C(132)	0.043 8(14)	0.367 1(11)	0.500 1(8)
C(11)	0.070 5(20)	0.255 6(18)	0.221 8(13)	C(133)	0.042 3(14)	0.427 5(11)	0.536 4(8)
C(12)	−0.005 6(17)	0.125 5(13)	0.237 3(9)	C(134)	−0.001 6(17)	0.417 6(12)	0.583 7(9)
C(13)	0.152 1(15)	0.158 0(11)	0.288 0(7)	C(135)	−0.038 1(14)	0.349 7(12)	0.598 2(8)
C(14)	−0.080 7(19)	0.254 0(15)	0.278 2(10)	C(136)	−0.027 7(14)	0.291 2(11)	0.564 5(8)
C(21)	0.159 8(19)	0.388 3(15)	0.265 3(11)	P(2)	−0.013 7(4)	0.134 4(3)	0.355 7(2)
C(22)	0.164 6(14)	0.431 3(11)	0.362 2(8)	C(211)	−0.133 8(15)	0.115 4(13)	0.366 1(9)
C(23)	0.005 0(19)	0.392 8(14)	0.322 1(9)	C(212)	−0.183 2(40)	0.088 3(37)	0.329 4(20)
C(24)	0.233 2(19)	0.292 9(14)	0.340 2(9)	C(213)	−0.285 1(23)	0.801 (19)	0.344 7(12)
P(1)	0.028 3(3)	0.219 6(2)	0.473 7(2)	C(221)	0.043 2(16)	0.047 7(12)	0.370 8(9)
C(111)	−0.066 9(11)	0.164 4(9)	0.490 5(6)	C(222)	0.033 5(21)	−0.007 7(15)	0.330 0(11)
C(112)	−0.151 3(13)	0.196 4(11)	0.485 9(7)	C(223)	0.076 1(27)	−0.078 1(19)	0.342 0(13)
C(113)	−0.228 7(16)	0.154 3(11)	0.495 7(8)				

Table 8 Fractional atomic coordinates for complex **10**

Atom	*X/a*	*Y/b*	*Z/c*	Atom	*X/a*	*Y/b*	*Z/c*
Pt(1)	0.298 64(7)	0.253 19(6)	0.121 47(6)	C(212)	0.027 3(23)	0.382 0(19)	0.057 2(16)
Pt(2)	0.504 49(7)	0.231 33(6)	0.133 01(5)	C(213)	−0.013 3(31)	0.439 2(26)	0.101 3(22)
Re(1)	0.393 17(8)	0.189 31(7)	0.231 55(6)	C(214)	0.038 8(23)	0.504 7(18)	0.105 8(16)
Re(2)	0.385 17(8)	0.138 69(6)	0.077 66(6)	C(215)	0.122 5(22)	0.490 1(17)	0.144 8(15)
P(1)	0.312 6(5)	0.298 6(4)	0.225 5(4)	C(216)	0.172 9(20)	0.433 7(16)	0.104 7(14)
P(2)	0.186 4(6)	0.300 9(4)	0.056 6(4)	C(221)	0.228 4(26)	0.329 3(21)	0.029 8(18)
P(3)	0.645 4(5)	0.265 1(4)	0.109 1(4)	C(222)	0.155 0(26)	0.361 0(20)	0.077 6(19)
O(11)	0.558 3(14)	0.277 0(12)	0.277 5(10)	C(223)	0.194 1(25)	0.363 5(20)	0.147 0(18)
O(12)	0.504 4(16)	0.057 1(13)	0.236 7(11)	C(224)	0.273 6(34)	0.408 1(28)	0.142 0(25)
O(13)	0.422 7(18)	0.206 2(14)	0.383 7(13)	C(225)	0.347 5(29)	0.374 3(23)	0.096 2(21)
O(14)	0.231 0(19)	0.098 2(16)	0.249 3(13)	C(226)	0.306 7(25)	0.368 3(19)	0.023 5(18)
O(21)	0.515 3(17)	0.022 2(14)	0.082 8(12)	C(231)	0.104 1(26)	0.238 7(20)	0.034 6(18)
O(22)	0.351 0(16)	0.111 4(13)	−0.074 1(12)	C(232)	0.129 5(23)	0.181 1(18)	0.014 3(17)
O(23)	0.486 3(17)	0.236 5(13)	−0.022 2(12)	C(233)	0.054 7(40)	0.126 9(31)	0.034 9(28)
O(24)	0.238 8(16)	0.037 9(13)	0.109 0(11)	C(234)	0.028 4(28)	0.098 2(22)	0.031 7(20)
C(11)	0.511 4(16)	0.247 8(12)	0.237 2(11)	C(235)	−0.004 6(36)	0.150 8(29)	0.085 5(26)
C(12)	0.467 0(19)	0.109 3(15)	0.227 8(14)	C(236)	0.073 9(30)	0.206 7(24)	0.098 4(21)
C(13)	0.410 5(20)	0.197 4(16)	0.327 1(14)	C(311)	0.711 9(19)	0.189 6(15)	0.087 5(14)
C(14)	0.286 1(20)	0.137 9(16)	0.236 9(15)	C(312)	0.681 4(23)	0.155 6(18)	0.021 6(17)
C(21)	0.468 6(19)	0.066 9(15)	0.085 0(13)	C(313)	0.753 4(27)	0.100 3(22)	0.003 7(26)
C(22)	0.365 4(18)	0.118 1(14)	−0.015 1(13)	C(314)	0.747 9(34)	0.042 3(28)	0.059 0(23)
C(23)	0.474 1(20)	0.219 3(16)	0.037 8(14)	C(315)	0.774 0(31)	0.071 4(26)	0.131 6(22)
C(24)	0.291 7(15)	0.075 7(20)	0.100 6(17)	C(316)	0.708 4(27)	0.137 7(21)	0.148 3(19)
C(111)	0.381 2(20)	0.377 4(16)	0.237 1(14)	C(321)	0.709 4(20)	0.305 0(16)	0.182 9(14)
C(112)	0.398 1(22)	0.399 2(18)	0.303 9(16)	C(322)	0.810 9(24)	0.305 2(20)	0.178 5(18)
C(113)	0.460 6(36)	0.469 0(24)	0.310 8(26)	C(323)	0.855 2(18)	0.334 1(23)	0.250 0(20)
C(114)	0.479 9(29)	0.492 1(23)	0.259 4(22)	C(324)	0.817 6(26)	0.409 1(21)	0.259 8(18)
C(115)	0.465 6(25)	0.466 4(20)	0.187 4(18)	C(325)	0.710 3(27)	0.409 0(21)	0.263 8(20)
C(116)	0.409 9(22)	0.406 5(17)	0.182 2(16)	C(326)	0.676 2(23)	0.380 8(18)	0.192 3(17)
C(121)	0.216 0(21)	0.320 4(16)	0.272 7(15)	C(331)	0.647 3(20)	0.319 0(16)	0.034 1(14)
C(122)	0.166 7(32)	0.258 7(25)	0.290 4(26)	C(332)	0.586 0(21)	0.379 8(17)	0.030 5(15)
C(123)	0.070 2(35)	0.277 2(17)	0.324 3(13)	C(333)	0.580 2(25)	0.411 0(20)	0.044 5(18)
C(124)	0.062 6(25)	0.338 7(21)	0.343 4(18)	C(334)	0.672 9(27)	0.436 4(22)	0.059 0(19)
C(125)	0.114 5(17)	0.398 6(22)	0.327 7(20)	C(335)	0.734 4(24)	0.372 0(19)	0.060 8(18)
C(126)	0.196 5(11)	0.389 3(18)	0.287 3(15)	C(336)	0.746 0(24)	0.341 2(20)	0.009 7(17)
C(211)	0.127 9(23)	0.374 9(18)	0.098 7(17)				

peaks not resolvable from those of **5a**, **6a** and $[Pt_3(CO)_3\{P(C_6H_{11})_3\}_3]$. NMR data, see Table 1.

Reaction of $[Re_2(CO)_9(PPr_2H)]$ with excess $[Pt(C_2H_4)_2\{P(C_6H_{11})_3\}]$ in CD_2Cl_2 (NMR monitoring) gave resonances assignable to **8b** (Table 1) together with additional resonances which have been assigned *tentatively* to $[Pt_2Re_2(\mu\text{-}PPr_2)(\mu\text{-}H)(\mu\text{-}CO)_3(CO)_6\{P(C_6H_{11})_3\}_2]$ **9**. NMR: ^1H, δ −11.0 [$^1J(^{195}Pt^1H)$ 759, $^2J(^{195}Pt^1H)$ 44, $J(^{31}P^1H)$ 15 Hz, μ-H]; $^{31}P\text{-}\{^1H\}$, δ 93 [$J(^{195}Pt^{31}P)$ 52, $J(^{31}P^{31}P)$ 6 Hz, μ-P] and 73 [$^1J(^{195}Pt^{31}P)$ 4370, $^2J(^{195}Pt^{31}P)$ 252, $^2J(^{195}Pt^{31}P)$ 6 Hz, $P(C_6H_{11})_3$].

$[Pt_2Re_2(\mu\text{-}PPh_2)(\mu\text{-}H)(\mu\text{-}CO)_2(CO)_6\{P(C_6H_{11})_3\}_2]$ **10**. To

Table 9 Fractional atomic coordinates for complex **12**

Atom	X/a	Y/b	Z/c	Atom	X/a	Y/b	Z/c
Pt(1)	0.149 33(5)	0.250 21(4)	0.117 38(4)	C(116)	−0.095 6(21)	0.134 9(14)	0.176 1(14)
Pt(2)	0.291 81(6)	0.240 06(4)	0.309 96(6)	C(121)	−0.136 3(16)	0.341 9(11)	0.065 4(11)
Re(1)	0.340 25(6)	0.359 22(4)	0.198 20(4)	C(122)	−0.274 0(16)	0.353 6(11)	0.017 6(11)
Re(2)	0.363 78(6)	0.161 88(4)	0.108 78(4)	C(123)	−0.311 1(20)	0.443 3(13)	0.025 3(13)
C(1)	0.334 1(16)	0.481 8(11)	0.197 6(10)	C(124)	−0.280 6(21)	0.468 9(15)	0.117 8(14)
O(1)	0.318 0(14)	0.556 9(10)	0.195 8(9)	C(125)	−0.151 1(13)	0.459 3(15)	0.169 2(16)
C(2)	0.500 1(17)	0.368 4(12)	0.277 7(12)	C(126)	−0.109 8(19)	0.366 2(12)	0.160 2(12)
O(2)	0.597 9(16)	0.384 2(10)	0.328 9(10)	C(131)	−0.095 1(11)	0.238 7(11)	0.074 2(11)
C(3)	0.396 5(16)	0.359 4(11)	0.098 4(11)	C(132)	−0.062 7(20)	0.153 0(13)	−0.104 7(13)
O(3)	0.433 5(14)	0.365 7(16)	0.039 2(10)	C(133)	−0.102 7(21)	0.151 7(14)	−0.206 6(13)
C(4)	0.396 3(17)	0.173 3(12)	0.072 5(12)	C(134)	−0.043 9(24)	0.223 2(15)	−0.239 5(16)
O(4)	0.410 1(16)	0.175 6(11)	0.004 8(11)	C(135)	−0.076 4(24)	0.310 4(16)	−0.208 0(15)
C(5)	0.395 9(19)	0.041 4(13)	0.179 6(13)	C(136)	−0.038 2(22)	0.311 0(15)	−0.107 9(14)
O(5)	0.409 7(17)	0.032 3(11)	0.176 1(11)	C(211)	0.149 3(19)	0.294 6(13)	0.464 1(12)
C(6)	0.530 0(20)	0.186 7(13)	0.242 2(13)	C(212)	0.027 4(22)	0.275 0(16)	0.395 5(16)
O(6)	0.633 8(17)	0.198 7(11)	0.276 7(11)	C(213)	−0.060 6(30)	0.345 3(20)	0.406 8(20)
C(1μ)	0.254 3(16)	0.372 0(11)	0.302 3(10)	C(214)	−0.069 1(27)	0.352 8(20)	0.495 0(18)
O(1μ)	0.204 3(12)	0.420 8(8)	0.330 9(8)	C(215)	0.049 8(28)	0.365 0(19)	0.561 3(20)
C(2μ)	0.155 0(14)	0.379 3(10)	0.109 5(10)	C(216)	0.134 2(23)	0.285 6(15)	0.555 3(15)
O(2μ)	0.103 2(12)	0.441 0(8)	0.070 0(8)	C(221)	0.415 8(17)	0.268 2(11)	0.527 3(12)
C(3μ)	0.175 5(17)	0.119 6(12)	0.111 0(11)	C(222)	0.526 4(20)	0.224 9(14)	0.520 4(14)
O(3μ)	0.125 5(15)	0.057 6(10)	0.078 4(10)	C(223)	0.644 3(25)	0.261 1(17)	0.580 6(18)
C(4μ)	0.320 2(21)	0.117 0(14)	0.293 9(14)	C(224)	0.658 1(23)	0.353 4(15)	0.576 6(16)
O(4μ)	0.315 8(19)	0.044 7(13)	0.327 1(13)	C(225)	0.551 5(23)	0.401 4(16)	0.585 1(16)
P(1)	0.058 1(4)	0.243 1(3)	0.046 6(3)	C(226)	0.426 4(20)	0.369 9(13)	0.519 5(14)
P(2)	0.275 6(4)	0.226 8(3)	0.448 5(3)	C(231)	0.270 2(12)	0.112 5(12)	0.483 8(12)
C(111)	−0.128 2(16)	0.142 6(11)	0.077 7(11)	C(232)	0.148 8(20)	0.067 3(14)	0.438 5(14)
C(112)	−0.261 7(14)	0.127 6(13)	0.031 8(13)	C(233)	0.161 8(27)	−0.028 6(17)	0.456 1(17)
C(113)	−0.300 4(21)	0.036 3(14)	0.051 7(14)	C(234)	0.197 8(24)	−0.048 6(16)	0.555 5(16)
C(114)	−0.264 9(23)	0.021 3(16)	0.152 4(15)	C(235)	0.311 1(23)	−0.000 3(15)	0.601 8(15)
C(115)	−0.139 6(21)	0.039 5(14)	0.195 4(14)	C(236)	0.301 2(20)	0.097 2(13)	0.582 3(13)

a solution of **6a** (0.14 g) in freshly distilled CH_2Cl_2 (5 cm^3) was added $[Pt(C_2H_4)_2\{P(C_6H_{11})_3\}]$ (0.275 g; 2.8 molar equivalents). The solution was allowed to stand for 1 week. Addition of hexanes gave an orange precipitate which on recrystallization from CH_2Cl_2–hexane gave **10** as orange-red plates (0.16 g) suitable for X-ray crystallography. IR (CH_2Cl_2): ν(CO) 2033s, 1992s, 1956m, 1925w(br), 1837w and 1785w cm^{-1}.

NMR monitoring of the reaction of **6a** with 1.4 molar equivalents of $[Pt(C_2H_4)_2\{P(C_6H_{11})_3\}]$ indicates initial formation of $[PtRe_2(\mu\text{-}PPh_2)(\mu\text{-}H)(CO)_8\{P(C_6H_{11})_3\}]$ **7c** (not isolated); NMR data, see Table 1.

$[Pt_2Re_2(\mu\text{-}CO)_4(CO)_6\{P(C_6H_{11})_3\}_2]$ **12**. To a solution of $[Re_2(CO)_{10}]$ (0.22 g) in dichloromethane (15 cm^3) was added 2 equivalents of $[Pt(C_2H_4)_2\{P(C_6H_{11})_3\}]$ (0.36 g). The solution was allowed to stand for 2 h. The volume of the solution was reduced (*in vacuo*) to *ca.* 3 cm^3 and hexane added. Complex **12** crystallized as orange prisms (0.41 g, 76% yield). IR (CH_2Cl_2): ν(CO) 2056s, 2011vs, 1979s, 1956m, 1853m, 1840m and 1802m cm^{-1} (Found: C, 34.30; H, 4.35; $C_{46}H_{66}O_{10}P_2Pt_2Re_2$ requires C, 34.45; H, 4.15%).

X-Ray Structure Determinations of **7b**, **10** *and* **12**.—Crystals of **7b** were pale yellow, those of **10** orange-red plates and those of **12** orange blocks and rhombs. All work was performed on an Enraf-Nonius CAD4 diffractometer by the use of graphite-monochromated Mo-Kα radiation. The resulting crystal data and the conditions used for the intensity measurements are summarized in Table 3. Lorentz, polarization corrections for crystal decay (**10** and **12**) and, at later stages of the refinements, absorption corrections were applied to all reflections collected. All three structures were solved using standard methods [Patterson (Pt and Re)] and refined by full-matrix (**7b**) or blocked (**10**) least-squares refinements (on ΔF minimizing $\Sigma w\Delta F^2$) to the indicated residuals, using Enraf–Nonius SDP[65] and SHELX[66] programs on PDP 11/23 and Gould 9705 computers respectively. For **10** H atoms were introduced in calculated positions. Scattering factors were taken from ref. 67. Tables 4–6 contain selected bond lengths and bond angles for all three compounds. Atomic coordinates are listed in Tables 7–9.

Additional material available from the Cambridge Crystallographic Data Centre comprises H-atom coordinates, thermal parameters and remaining bond distances and angles.

Acknowledgements

We thank the Natural Sciences and Engineering Research Council of Canada for financial support of this work.

References

1 D. A. Roberts and G. L. Geoffroy, in *Comprehensive Organometallic Chemistry*, eds. G. Wilkinson, F. G. A. Stone and E. W. Abel, Pergamon, Oxford, 1982, ch. 40.
2 H. J. Langenbach and H. Vahrenkamp, *Chem. Ber.*, 1979, **112**, 3773.
3 E. Sappa, A. Tiripicchio and P. Braunstein, *Coord. Chem. Rev.*, 1985, **65**, 219.
4 L. M. Venanzi, *Coord. Chem. Rev.*, 1982, **43**, 251.
5 A. P. Humphries and H. D. Kaesz, *Prog. Inorg. Chem.*, 1979, **25**, 145.
6 R. Shojaie and J. D. Atwood, *Inorg. Chem.*, 1987, **26**, 2199.
7 R. D. Adams and I. T. Horvarth, *Prog. Inorg. Chem.*, 1985, **33**, 127.
8 F. G. A. Stone, *Angew. Chem., Int. Ed. Engl.*, 1984, **23**, 89.
9 S. Rosenberg, S. P. Lockledge and G. L. Geoffroy, *Organometallics*, 1986, **5**, 2517.
10 S. Rosenberg, W. S. Mahoney, J. M. Hayes and G. L. Geoffroy, *Organometallics*, 1986, **5**, 1065.
11 S. J. Loeb, H. A. Taylor, L. Gelmini and W. D. Stephan, *Inorg. Chem.*, 1986, **25**, 1977.
12 L. Gelmini and W. D. Stephan, *Inorg. Chem.*, 1986, **25**, 1222.
13 T. S. Targos, B. P. Rosen, R. R. Whittle and G. L. Geoffroy, *Inorg. Chem.*, 1985, **24**, 1375.
14 R. T. Baker, T. H. Tulip and S. S. Wreford, *Inorg. Chem.*, 1985, **24**, 1379.
15 W. C. Mercer, G. L. Geoffroy and A. L. Rheingold, *Organometallics*, 1985, **4**, 1418.

16 W. C. Mercer, R. R. Whittle, E. W. Burkhardt and G. L. Geoffroy, *Organometallics*, 1985, **4**, 68.
17 J. Powell, C. Couture, M. R. Gregg and J. F. Sawyer, *Inorg. Chem.*, 1989, **28**, 3437.
18 S. Rosenberg, G. L. Geoffroy and A. L. Rheingold, *Organometallics*, 1985, **4**, 1184.
19 S. Rosenberg, R. R. Whittle and G. L. Geoffroy, *J. Am. Chem. Soc.*, 1984, **106**, 5934.
20 G. L. Geoffroy, S. Rosenberg, P. M. Shulman and R. R. Whittle, *J. Am. Chem. Soc.*, 1984, **106**, 1519.
21 M. J. Breen, P. M. Shulman, G. L. Geoffroy, A. L. Reingold and W. C. Fultz, *Organometallics*, 1984, **3**, 782.
22 E. W. Burkhardt, W. C. Mercer and G. L. Geoffroy, *Inorg. Chem.*, 1984, **23**, 1779.
23 E. D. Morrison, A. D. Harley, M. A. Morielli, G. L. Geoffroy, A. L. Rheingold and W. C. Fultz, *Organometallics*, 1984, **3**, 1407.
24 J. Powell, M. R. Gregg and J. F. Sawyer, *J. Chem. Soc., Chem. Commun.*, 1984, 1149.
25 J. Powell, M. R. Gregg and J. F. Sawyer, *Inorg. Chem.*, 1989, **28**, 4451.
26 J. Powell, M. R. Gregg and J. F. Sawyer, *J. Chem. Soc., Chem. Commun.*, 1987, 1029.
27 J. Powell, J. F. Sawyer and S. J. Smith, *J. Chem. Soc., Chem. Commun.*, 1985, 1312.
28 J. Powell, J. F. Sawyer and M. V. R. Stainer, *J. Chem. Soc., Chem. Commun.*, 1985, 1314.
29 J. Powell, J. F. Sawyer and M. V. R. Stainer, *Inorg. Chem.*, 1989, **28**, 4461.
30 J. Powell, E. Fuchs, M. R. Gregg, J. Phillips and M. V. R. Stainer, *Organometallics*, 1990, **9**, 387.
31 J. Powell, M. R. Gregg and J. F. Sawyer, *Inorg. Chem.*, 1988, **27**, 4526.
32 M. Bernard, A. Dedieu and S. Nakamura, *Nouv. J. Chim.*, 1984, **8**, 149; E. D. Jemmis, A. R. Pinhas and R. Hoffmann, *J. Am. Chem. Soc.*, 1980, **102**, 2576; M. Bernard, *J. Am. Chem. Soc.*, 1978, **100**, 7740; M. Bernard, *Inorg. Chem.*, 1979, **18**, 2782; R. Mason and D. M. P. Mingos, *J. Organomet. Chem.*, 1973, **50**, 53; R. H. Summerville and R. Hoffman, *J. Am. Chem. Soc.*, 1976, **98**, 7240; J. W. Lauher, M. Elain, R. H. Summerville and R. Hoffmann, *J. Am. Chem. Soc.*, 1976, **98**, 3219; M. R. Churchill, B. G. DeBoer and F. T. Rotella, *Inorg. Chem.*, 1976, **15**, 1843.
33 J. Powell, J. C. Brewer, G. Gulia and J. F. Sawyer, *Inorg. Chem.*, 1989, **28**, 4470.
34 M. C. Favas and D. L. Kepert, *Prog. Inorg. Chem.*, 1980, **27**, 325.
35 J. Powell, *J. Chem. Soc., Chem. Commun.*, 1989, 200.
36 H. J. Haupt, P. Balsaa and U. Florke, *Inorg. Chem.*, 1988, **27**, 280.
37 G. Ciani, M. Moret, A. Sironi, T. Beringhelli, G. D'Alfonso and R. D. Pergola, *J. Chem. Soc., Chem. Commun.*, 1990, 1668.
38 U. Koelle, *J. Organomet. Chem.*, 1978, **155**, 53.
39 B. F. G. Johnson, J. Lewis and D. A. Pippard, *J. Chem. Soc., Dalton Trans.*, 1981, 407.
40 W. Tam, G.-Y. Lin, W.-K. Wong, W. A. Kiel, V. K. Wong and A. J. Gladysz, *J. Am. Chem. Soc.*, 1982, **104**, 141.
41 D. R. Gard and T. L. Brown, *J. Am. Chem. Soc.*, 1982, **104**, 6340.
42 D. J. Cox and R. Davis, *J. Organomet. Chem.*, 1980, **186**, 339.
43 R. Giordano, E. Sappa, A. Tiripicchio, M. Tiripicchio Camellini, M. J. Mays and M. P. Brown, *Polyhedron*, 1989, **8**, 1855.
44 D. S. Moore and S. D. Robinson, *Chem. Soc. Rev.*, 1983, **12**, 415.
45 A. J. Carty, *Adv. Chem. Ser.*, 1982, **196**, 163.
46 S. R. Drake, B. F. Johnson and J. Lewis, *J. Chem. Soc., Chem. Commun.*, 1988, 1033.
47 M. R. Bradford, N. G. Connelly, N. C. Harrison and J. C. Jeffery, *Organometallics*, 1989, **8**, 1829.
48 T. Beringhelli, A. Ceriotti, G. D'Alfonso and R. D. Pergolla, *Organometallics*, 1990, **9**, 1053.
49 C. P. Casey, E. W. Rutter, jun. and K. J. Haller, *J. Am. Chem. Soc.*, 1987, **109**, 6886.
50 M. R. Churchill, K. N. Amoh and H. J. Wasserman, *Inorg. Chem.*, 1981, **20**, 1609.
51 R. Bau, B. Fontal, H. D. Kaesz and M. R. Churchill, *J. Am. Chem. Soc.*, 1967, **89**, 6374.
52 T. Yoshida, T. Yamagata, T. H. Tulip, J. A. Ibers and S. Otsuka, *J. Am. Chem. Soc.*, 1978, **100**, 2063.
53 R. Bender, P. Braunstein, J.-M. Jud and Y. Dusausoy, *Inorg. Chem.*, 1984, **23**, 4489.
54 L. J. Farrugia, J. A. K. Howard, P. Mitrprachachon, F. G. A. Stone and P. Woodward, *J. Chem. Soc., Dalton Trans.*, 1981, 1134.
55 L. J. Farrugia, J. A. K. Howard, P. Mitrprachachon, F. G. A. Stone and P. Woodward, *J. Chem. Soc., Chem. Commun.*, 1978, 260.
56 H. B. Davis, F. W. B. Einstein, V. J. Johnston and R. K. Pomeroy, *J. Am. Chem. Soc.*, 1988, **110**, 4451.
57 M. R. Churchill, B. G. DeBoer and F. J. Rotella, *Inorg. Chem.*, 1976, **15**, 1843.
58 R. G. Teller and R. Bau, *Struct. Bonding (Berlin)*, 1981, **44**, 1.
59 T. V. Ashworth, J. A. K. Howard, M. Laguna and F. G. A. Stone, *J. Chem. Soc., Dalton Trans.*, 1980, 1593.
60 R. A. Jones, J. G. Lasch, N. C. Norman, A. L. Stuart, T. C. Wright and B. R. Whittlesey, *Organometallics*, 1984, **3**, 114.
61 J. L. Spencer, *Inorg. Synth.*, 1979, **19**, 216.
62 D. M. Blake and D. M. Roundhill, *Inorg. Synth.*, 1978, **18**, 120.
63 H. Saltzman and J. G. Sharefkin, *Org. Synth.*, 1960, **43**, 60.
64 A. Moor, P. S. Pregosin and L. M. Venanzi, *Inorg. Chim. Acta*, 1981, **48**, 153.
65 B. A. Frenz, SDP Structure Determination Package, College Station, TX, 1982.
66 G. M. Sheldrick, SHELX 76 and 86, Programs for crystal structure determination and refinement, University of Cambridge, 1976 and 1986.
67 *International Tables for X-Ray Crystallography*, Kynoch Press, Birmingham, 1974, vol. 4.

Received 16*th December* 1991; *Paper* 1/06310C